

Self-Supervised Damage-Avoiding Manipulation Strategy Optimization via Mental Simulation

Tobias Fromm *

March 5, 2022

Abstract

Everyday robotics are challenged to deal with autonomous product handling in applications like logistics or retail, possibly causing damage on the items during manipulation. Traditionally, most approaches try to minimize physical interaction with goods. However, we propose to take into account any unintended motion of objects in the scene and to learn manipulation strategies in a self-supervised way which minimize the potential damage.


The presented approach consists of a planning method that determines the optimal sequence to manipulate a number of objects in a scene with respect to possible damage by simulating interaction and hence anticipating scene dynamics. The planned manipulation sequences are taken as input to a machine learning process which generalizes to new, unseen scenes in the same application scenario. This learned manipulation strategy is continuously refined in a self-supervised optimization cycle during load-free times of the system. Such a simulation-in-the-loop setup is commonly known as *mental simulation* and allows for efficient, fully automatic generation of training data as opposed to classical supervised learning approaches. In parallel, the generated manipulation strategies can be deployed in near-real time in an anytime fashion.

We evaluate our approach on one industrial scenario (autonomous container unloading) and one retail scenario (autonomous shelf replenishment).

Keywords: manipulation strategy optimization · damage-avoiding manipulation · mental simulation · simulation in the loop · autonomous container unloading · autonomous shelf replenishment

Supplementary Video: http://robotics.jacobs-university.de/TMP/jint_manipulation_strategy_optimization.mp4

Software: <https://github.com/jacobs-robotics/gazebo-mental-simulation> (see Section 5)

*Tobias Fromm  orcid.org/0000-0001-6488-8211 is with the Robotics Group, Computer Science & Electrical Engineering, Jacobs University Bremen, Germany; t.fromm@jacobs-university.de. The author would like to thank Christian A. Mueller for the fruitful discussions and valuable comments. The research leading to the presented results has received funding from the European Union's Seventh Framework program (EU FP7 ICT-2) within the project "Cognitive Robot for Automation of Logistics Processes" (RobLog).

1 Introduction

Since common perception and motion planning approaches have to deal with noisy sensor readings and cluttered environments, autonomous manipulation can be destructive if fragile goods have to be handled. Many compliant grippers, sophisticated perception systems and manipulation routines have been developed recently, mostly relying on consequent obstacle avoidance. This works to a certain degree, but we propose to take alteration of the environment into account instead of bluntly avoiding interaction with it.

In this work, we present a *manipulation strategy optimization* method which is able to select the best sequence to remove or unload a number of objects from a scene while taking into account possible damage-prone movements of any other objects. A *manipulation strategy*, in the first place, we define as a decision process which determines an optimal sequence in which to manipulate the scene objects with respect to application-specific optimization criteria. The generated strategies can be optimized autonomously by the robot during load-free times. This is achieved by generating and processing training data for learning preferences and physical constraints between the objects in a self-supervised way. We exploit a simulation-in-the-loop setup which utilizes a physics simulation to generate arbitrary amounts of training data, hence no user interaction is needed throughout the whole process as opposed to classical supervised learning approaches.

The proposed method relies on *mental simulation* of the movements of all objects present in the scene during manipulation, a term which originates from a psychology context with a first mention in [22]. In general, reasoning and drawing conclusions from a simulation process has been investigated in the literature under different terms, but altogether considering the dynamics of a scene in a human-like way. Battaglia et al. [3] introduced the term *intuitive physics engine* which describes the human anticipation capabilities from a cognition-scientific viewpoint. They find the quantitative evaluations of human reasoning capabilities to be surprisingly similar to the results obtained from physics simulations. Other well-known terminology is *temporal projection* [29], *physics-based reasoning* [2] and *physical reasoning* [57] which deal with predicting real-world behavior using knowledge inferred from physics simulation. In terms of repetitively performing actions which improve environment manipulation strategies, *robotic playing* [17] is another related bio-inspired technique which compares trial-and-error behavior while accumulating environment knowledge with a children’s way of exploring the world. In the case of our proposed method, we can add the term *dreaming robot* to this list of synonyms for mental simulation because the manipulation strategy optimization happens during load-free times, for instance at night when the robot is otherwise unused. Additionally, since the manipulation strategies generated inside our approach can be transferred to a real-world scenario, *transfer learning* is another applicable high-level term.

Fig. 1 shows an overview of our method. In order to obtain and optimize manipulation strategies, we track the dynamics of the scene using a physics simulation. This contains a copy of the physical scene, including a robot, the environment and a number of objects to manipulate, defined domain-specificly depending on the application (Fig. 1 top left). In order to allow for generalization of these mental simulation capabilities, we automatically generate training scenes (top center) which, after determining the respective optimal manipula-

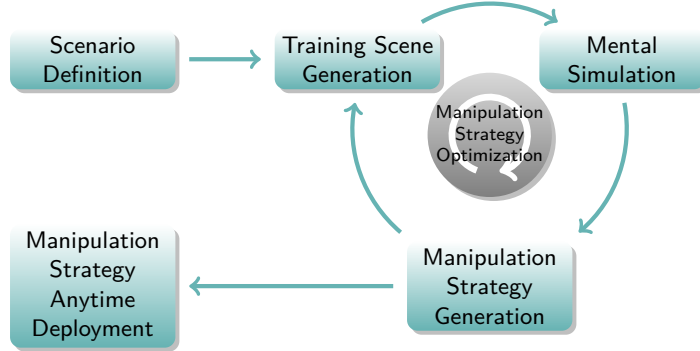


Figure 1: Overview of the proposed method

Nodes are clickable and linked to the respective sections in this paper. This diagram reappears in every section to allow for easy orientation within our method.

tion sequence in terms of minimizing undesired object motion, serve as training examples for a machine learning process (top right). Once a number of training samples has been acquired, a classifier is built and updated iteratively on new incoming samples, yielding an updated manipulation strategy (bottom right). Subsequently, the resulting classifier can, over the course of many simulated manipulation procedures, be deployed to predict manipulation sequences with respect to the learned strategy from any new scene (bottom left).

The possibilities are manifold: One the one hand, motion planning within our method is facilitated because of a less constrained search space in contrast to regarding all other objects as obstacles. In some scenes, it may be hard or even impossible to perform manipulation if no collisions are permitted using conventional approaches like our previous work [49]. On the other hand, because the necessary training data can be generated and consumed in a self-supervised manner by running simulations of manipulation actions, the resulting strategy can be optimized during load-free times. Parallelizing the simulation process makes the actual manipulation very efficient because the strategy improves quickly and can be applied instantly, without the need for any more simulation or other processing. Additionally, since strategy optimization happens in the background without dependencies on the real scene, the currently active strategy can be deployed *anytime* in *near-real time* without the need to synchronize the learning process with physical robot behavior.

The main motivation of our approach is to avoid damage to the possibly heavy or fragile goods as well as the robot itself which may occur if an object is shifted or dropped unintendedly. However, detecting actual physical damage on handled goods has to be regarded as an own field of research related to object recognition and classification. In the scope of our work, we hence define damage avoidance as an implicit, proactive way of minimizing unintended motion of objects during the manipulation process.

In any case, although the goal of our method is to optimize the autonomous behavior of a robot according to the anticipated dynamics of the real-life scene, we do not impose any explicit spatial or logical dependencies between objects. In addition, our method includes no priors about the type and size of objects, degrees of freedom of the robot, type of manipulator or other application domain-

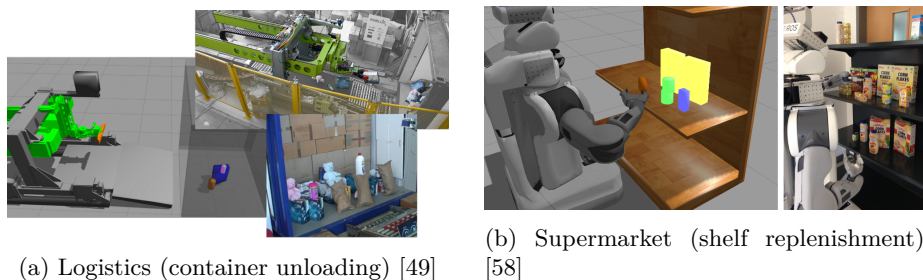


Figure 2: Typical application scenarios for autonomous manipulation [11]

specific parameters. Hence it is not tied to a particular application domain and can be deployed on new scenarios within minimal time, given that a working simulation of the manipulation procedures to be sequenced has been established already.

One of our main contributions is the integration of the simulation into the processing loop which is essential for our self-supervised mental simulation approach. Another example where simulation in the loop may play an important role is system integration which this way can be conducted as a continuous process. Hence, parts of the system can be tested individually using simulated components and gradually replaced by their real-world counterparts. Such a continuous system integration [13] technique uses simulation in the same way, embedded into a closed loop and as a full-featured component which seamlessly integrates into the processing pipeline.

All of the different terminology mentioned so far share the common ground of mentally simulating robot interaction in dynamic environments, but have been applied to a multitude of different domains. In order to show the general applicability of our approach which is not limited to a particular domain, we use two different everyday scenarios shown in Figure 2: *logistics*, in the context of the EU project “Cognitive Robot for Automation of Logistics Processes” (RobLog)¹ [49] where containers are unloaded autonomously, and in a *supermarket* environment for autonomous shelf replenishment [58].

As for the first scenario, many heavy, bulky, fragile or otherwise damage-prone goods are handled in logistics. Especially in terms of relieving human workers from health-endangering labor, robotic applications have been flourishing in this domain for several years. Our work on unloading shipping containers provides an ideal application in this respect, so we have modeled the robot, container and objects from this scenario as our first example.

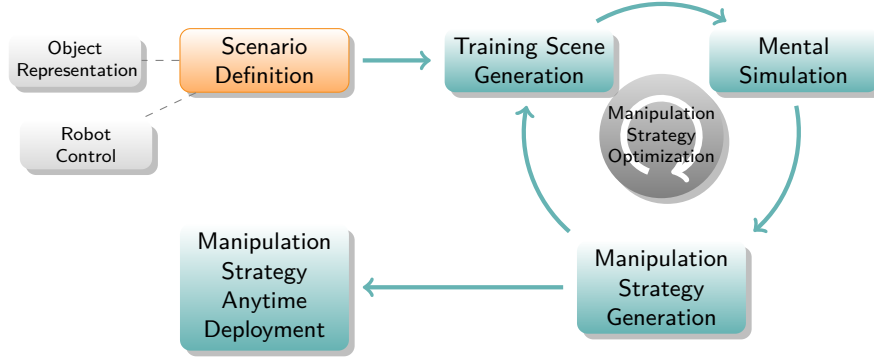
Secondly, interleaved with logistics in terms of hardware and software transitioning from one field to the other, but still facing different challenges, domestic and retail robotics provide another playground for manipulation strategy optimization. As a concrete scenario, we will use a supermarket scenario featuring a PR2 robot as a second application example.

¹<http://roblog.eu>

2 Prerequisites

First of all, before explaining our method in detail, this section gives a short overview about certain prerequisites that have to be considered as given when deploying our method. This includes the initial definition of the scene with respect to the particular usage scenario as well as how to auto-generate a large number of scenes used within the manipulation strategy optimization cycle.

2.1 Scenario definition



Simulating the behavior of robots and objects requires both high accuracy and a certain amount of abstraction since not every detail in robot and object properties can be modeled easily. Our approach is intended to work in integrated scenarios based on perception systems for object recognition and real robots for motion execution. In order to interact with such components while still focusing on the simulation of complex scenes, we do not address noise and inaccuracies of other pipeline components in this work. Hence, we assume object models and environment to be given as well as the state of the robot.

2.1.1 Object representation

As for representation the scene objects in simulation, it is generally desired to obtain detailed models of them in order to achieve realistic dynamic behaviors. However, detailed object models generated from a real object’s point cloud like in our previous work [12] introduce the tradeoff of instable initial scenes in the physics simulation due to modelling inaccuracies. This may lead to some objects shifting immediately after spawning them in the physics engine. This has to be avoided for mentally simulating manipulation actions since initially stable scenes in the physics simulation represent reality where, during and after object recognition, objects most likely are not transposed either if not physically influenced. In order to preserve stable initial configurations, the proposed method therefore uses abstract object representations as shown in Fig. 3 in order to avoid modeling errors.

During productive use in a concrete application scenarios, the respective scene configuration needs to be established in the physics simulation. This requires to recognize and localize objects occurring in the scene; for our use cases we utilize the perception system originally developed for the logistics scenario [49, 53]. This system includes a pipeline of several segmentation and filtering

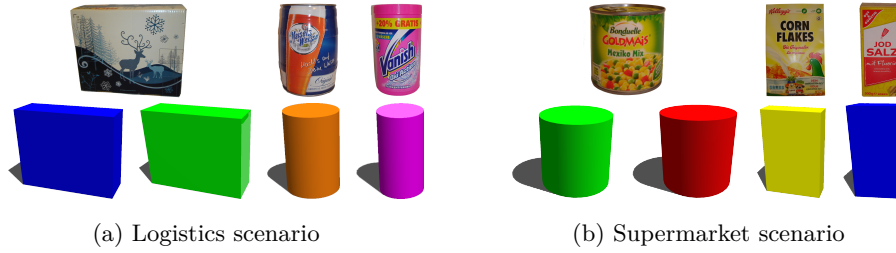


Figure 3: Objects and their simulation representations (not drawn to scale)

steps before it executes diverse recognition modules, including a feature-based textured object recognition module [55] and a graph-based shape model recognition module [37].

2.1.2 Robot control

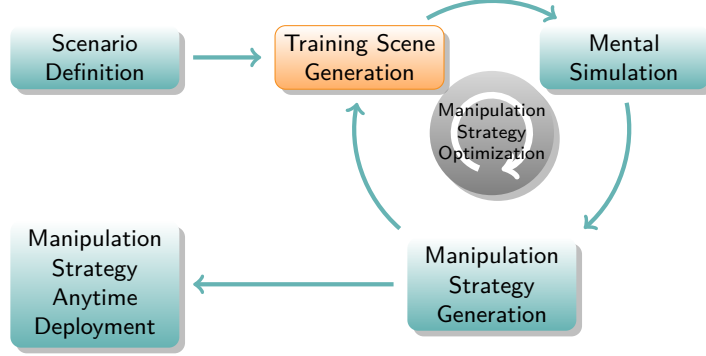
After all objects have been perceived, the respective grasps need to be planned, evaluated and finally executed by the robot. The way of determining grasping configurations strongly depends on the objects and gripper used in the scenario since different object dimensions and structure demand for different gripper sizes and amounts of dexterity. Since the focus in this work does not lie on grasp and motion planning and our method is supposed to be re-used in different scenarios, we use generic grasping configurations around the principal object axes.

The physics simulation uses a kinematics and dynamics model of the robot which has been developed together with the respective simulated controllers. The container unloading robot in the logistics scenario (Fig. 2a) uses a custom set of low-level and high-level controllers. For the supermarket scenario (Fig. 2b), we use the standard PR2 simulation model. The eventual generation of motion trajectories can be performed by using a standard motion planner like the ones integrated in the Open Motion Planning Library² [50].

Being equipped with scenes containing environment, objects and a fully functional robot, the physics simulation can now be utilized to perform plan manipulation sequences using mental simulation. This, together with a methodology how to take care of possible damage, will be explained in the following section.

²<http://ompl.kavrakilab.org/>

2.2 Training scene generation



One important part of the proposed method includes the robot using load-free times to optimize its manipulation strategies. This includes re-training the respective Machine Learning algorithms, but also the generation of additional training data. In order to be ready for unloading many possible combinations of objects in different spatial relationships, we generate training scenes with configurations where objects are likely to collide with or obstruct other objects. This happens by spawning the objects in clusters defined by their x, y, z size in the predefined workspace (e.g. inside a container, on a specific shelf level). Random cluster centroids are then drawn from the workspace volume around which the objects are located with random 6-D poses.

For refining the object poses and removing any interpenetrations that may have occurred, we use PROMTS³ [34] which translates any given object configuration in space to a collision-free configuration. Battaglia et al. [3] use the same principle that helps generating scenes which incorporate a certain amount of noise, but still are conceivable as per human intuition and the physics simulation.

Figure 4 shows some examples for both our scenarios. In fact, we create several variations of each scene with stochastic noise added to the object poses which are superimposed in the examples. Whenever new training scenes have been generated, they are provided as input for the training data extraction process as described in the next section.

³<https://github.com/Rasoul77/prompts>

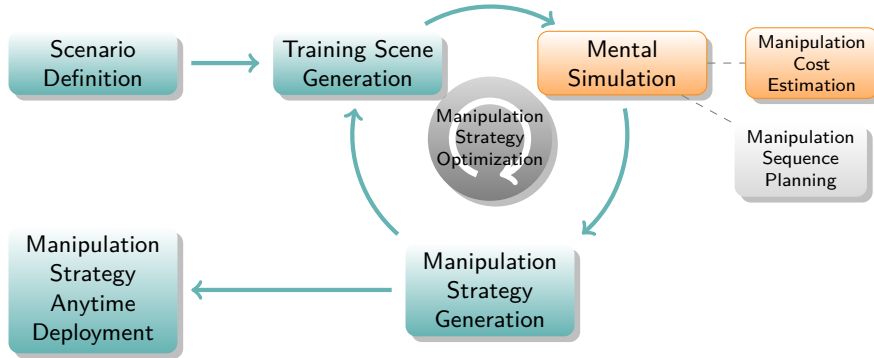
tion if no collisions are permitted. On the other hand, we want to avoid damage to the possibly heavy or fragile goods as well as to the robot itself which may occur if an object is shifted or dropped unintendedly. Hence, the goal of our manipulation sequence planning approach is to optimize a robot’s autonomous behavior according to the anticipated dynamics of the real-world scene.

In the literature, an effective example of motion planning for a humanoid robot was presented by Okada et al. [38] where obstacles are considered as planning goals and subsequently moved away from the desired walking path. Their goal is to enable robots to implicitly perform necessary manipulation actions, even if these actions were not part of the original task plan. This is similar to our recent work evaluated in a different scenario [58], but different to what we present in this work. Here we use a dynamics simulation to evaluate the feasibility of a manipulation action, taking unintended side effects into account in addition to static spatial knowledge.

Kitaev et al. [26] and Dogar et al. [8] present methods of planning grasps through clutter, taking shifting objects into account and explicitly manipulating them. The objective of this is partly similar to our approach, though not with the intention to find an efficient manipulation order, but to clear manipulation paths from obstructing objects. On the other hand, Stilman et al. [48] explicitly plan which objects to move away and where to move them in order to reach a target object. In the contrary, our collision-agnostic approach mitigates excessive motion planning times which occur in the context of collision avoidance.

For all of the following definitions, we use \mathcal{O} as the set of objects present in the scene, $\alpha \in \mathcal{O}$ as the *active object* (that will be manipulated), $\Phi = \mathcal{O} \setminus \alpha$ as the set of *passive objects* (that will not be manipulated) and $\phi \in \Phi$ as one member of this set.

3.1 Manipulation cost estimation



The usage of cost functions to find the most suitable and reasonable solution to a planning problem has been common practice for a long time (e.g. in [14, 38]) to be able to evaluate the effects of a particular action. In order to apply this method to a specific planning problem, domain knowledge has to come into play which accounts for the optimization target of the respective problem.

Since our approach aims on reducing unintended motions of *passive objects*, i.e. objects which are not subject to intended manipulation at the moment,

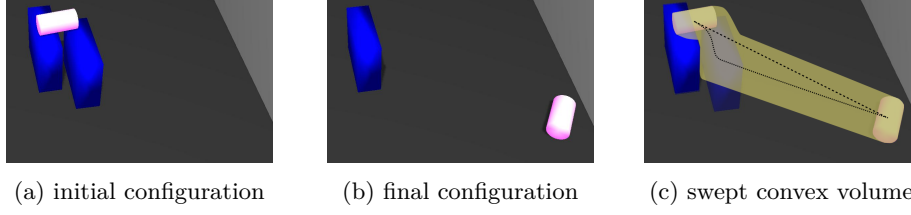


Figure 5: Visualization of the swept convex volume covered by a passive object during manipulation. When the right blue block is pulled out by the robot, the cylindrical pink object falls down and rolls away following the yellow path.

we need to consider a cost function which covers spatial modifications in the scene. However, in order to consider complex motion paths as well as changes of movement direction and spin, generic Euclidean distance-based or trajectory length-based cost functions do not deliver accurate cost estimates. Instead, we propose to use a *swept volume*-based representation of the object motion costs.

Generally, swept volume estimations can be used for collision detection [52] as well as space occupancy calculation, e.g. for automation and production [9]. For a mathematical formulation see the survey of Abdel-Malek et al. [1]. The object’s surface is used as the *generator* which follows a *trajectory* (a set of poses covered while moving during simulation runtime) and creates the *swept volume* (the outer boundary of the object during its motion). This can be considered a voxel-based variant of [1], widely used in applications where generator and trajectory are discrete.

In most applications, this volume basically represents a concave hull around all points in space which the object ever touched. However, this takes a lot of effort to compute [9] and, since the concave hull of a number of points is not generally well-defined, may raise ambiguities for different kinds of objects. As a remedy, we simplified the original swept volume approach by replacing the concave with the convex hull, normalized by object volume, which is easy to compute and well-defined, and call the result the *swept convex volume* (see Figure 5).

Since all objects in a scene shall be regarded when computing manipulation costs, we take the *maximum swept convex volume* V_{max} which is the maximum over all swept convex volumes of the scene objects. It is determined as

$$V_{max} = \max_{\phi \in \Phi} V_s(\phi) \quad (3.1)$$

where $V_s(\phi)$ is the swept convex volume of the $\phi \in \Phi$ as computed in Algorithm 1.

Algorithm 1 Swept convex volume calculation

- 1: **input:** object mesh $\mathcal{M}(\phi)$, object poses $\mathbf{p}_{0..n}(\phi)$ covered during simulation
 - 2: create point cloud $\mathcal{C}(\phi)$ from $\mathcal{M}(\phi)$ at $\mathbf{p}_0(\phi)$
 - 3: **for all** $\mathbf{p}_i(\phi)$ **do**
 - 4: $\mathcal{C}_i(\phi) \leftarrow \mathcal{C}(\phi)$ transformed from $\mathbf{p}_0(\phi)$ to $\mathbf{p}_i(\phi)$
 - 5: $\mathcal{C}(\phi) \leftarrow \mathcal{C}(\phi) \cup \mathcal{C}_i(\phi)$
 - 6: **end for**
 - 7: $H(\phi) \leftarrow \text{convhull}(\mathcal{C}(\phi))$
 - 8: $H_0(\phi) \leftarrow \text{convhull}(\mathcal{C}_0(\phi))$
 - 9: $V_s(\phi) \leftarrow \text{volume}(H(\phi)) / \text{volume}(H_0(\phi))$
 - 10: **output:** swept convex volume $V(\phi)$
-

Since the desired usage of our method puts special focus on fragile and vulnerable goods, we propose to employ additional weights for each component of the 6-D pose to V_{max} , calling the resulting cost function the *maximum weighted swept convex volume* V_w . These weights can be adapted to the domain, e.g. to sanction vertically dropping objects like when they fall off a shelf or out of a container. Additionally, one could think of applications like objects placed on a running conveyor belt where a lateral translation could push the goods off the belt, thus stopping them to be conveyed. Rotational weights may be employed in a domain dealing with objects which spill when they are turned, for example liquid containers or generally any container which is open on its top.

As for the parameterization of such weights, in Algorithm 1 we need to replace $\mathbf{p}_i(\phi)$ in Line 4 with the weighted $\mathbf{p}_i^w(\phi)$:

$$\mathbf{p}_i^w(\phi) = \mathbf{p}_0(\phi) + \text{diag}(\mathbf{w}) \cdot (\mathbf{p}_i(\phi) - \mathbf{p}_0(\phi)) \quad (3.2)$$

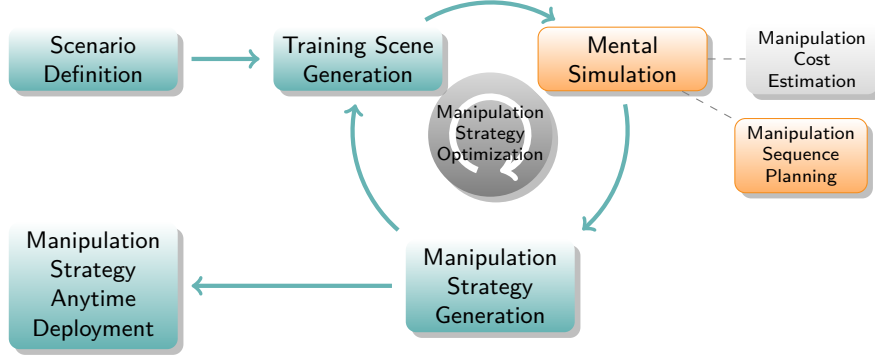
where $\mathbf{w} = [w_x \ w_y \ w_z \ w_\varphi \ w_\theta \ w_\psi]^\top$ are domain-dependent weights for each of the components of the 6-D object pose.

Projecting this to our general approach which is not limited to scenarios where damage-awareness is the main focus, we still want to emphasize the importance of this factor in our concrete application scenarios. Thus, we set the weights on

$$\mathbf{w} = [1 \ 1 \ 2 \ 1 \ 1 \ 1]^\top$$

which puts emphasis on damage-prone vertical motion. This is desired especially in scenarios like a supermarket where objects would break if dropped from a shelf.

3.2 Damage-avoiding manipulation sequence planning



Using mental simulation of a robot’s interaction with a scene as a validation method for planned actions can be used in runtime-restricted scenarios and scenarios where another planner has already determined which objects to manipulate in which order. One example for this is the planner presented by Mojta-hedzadeh et al. [33] which uses static equilibrium calculations to find objects that support each other, hence it will eventually select objects first which do not support any other object. Implicitly, our manipulation sequence planning method will usually determine similar manipulation sequences, but in addition considers dynamic events occurring during the manipulation for which Mojta-hedzadeh et al.’s approach is not equipped. Consequently, using our method for

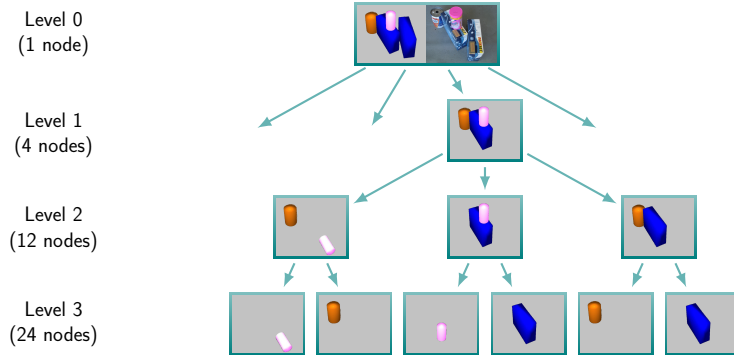


Figure 6: Example search tree

Some branches cropped for increased visibility. Each node shows its initial configuration, i.e. prior to manipulation.

validating plans on dynamic scenarios can be seen as an addition and enrichment to another planner.

In general, mentally simulated interaction can be used as a validation method which outputs the manipulation costs for a given scene configuration. In order to deduce the next action for the robot to be performed, however, classification between positively and negatively validated actions has to be performed somehow. Naively, this can be achieved by modeling specific thresholds for the manipulation costs.

This is a common problem for physics-based validation methods in general, e.g. for Rockel et al.’s approach [43] where thresholds are defined manually for which an object is considered to be toppling. Another example is [40] where the authors perform statistical tests on whether a planned motion lies within a learned envelope. Whenever such an approach is deployed on a new scenario, these parameters have to be set accordingly. However, in the vast majority of deployment settings, classification between actions causing positive and negative results in the respective context has to happen automatically. The user should not have to predefine thresholds and parameters in order to be adaptable to changing scenarios and environments.

In the usage example of avoiding damage by unintentionally moving objects, our method is able to plan a manipulation sequence which considers these side-effects. In addition, obstacle-avoiding motion planning may fail in certain scenarios due to an overly complex motion planning problem in confined spaces. But since we explicitly allow for moving passive objects during manipulation, though trying to minimize it, our high-level planner may still succeed in finding a viable manipulation sequence.

In our previous work [49], we have sketched the difficulties and pitfalls of classical motion planning in heavily confined spaces, i.e. when all passive objects are considered as obstacles. This may even lead to a dead end in manipulating any remaining object if the constraints are too tight. Manipulation sequence planning exploiting object dynamics, on the other hand, allows for passive objects to move and takes their motion into account as a feature, thus getting stuck in such a case is less likely.


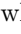
Our method uses a *search tree* built from all possible objects configurations which can occur while manipulating all objects in the scene. Such a tree-search

Algorithm 2 Search tree generation for manipulation sequence planning

```
1: initialize search tree  $\mathcal{S}_0 \leftarrow \emptyset$ 
2: initialize set of objects  $\mathcal{O}_0$  with current scene
3: procedure  $\text{CREATE\_NODE}(\mathcal{S}_i, \mathcal{O}_i)$ 
4:   if  $|\mathcal{O}_i| \leq 1$ , i.e. this is a leaf node then
5:     return
6:   else
7:     create new tree node  $N_i$  containing object set  $\mathcal{O}_i$ 
8:      $\mathcal{S}_{i+1} \leftarrow \mathcal{S}_i \cup N_i$ 
9:     determine new active object  $\alpha_i \in \mathcal{O}_i$ 
10:     $\mathcal{O}_{i+1} \leftarrow \mathcal{O}_i \setminus \alpha_i$ 
11:    return  $\text{CREATE\_NODE}(\mathcal{S}_{i+1}, \mathcal{O}_{i+1})$ 
12:   end if
13: end procedure
14: output: filled search tree  $\mathcal{S}$ 
```

Algorithm 3 Manipulation sequence planning for mental simulation

```
1: input: scene objects  $\mathcal{O}$ , search tree  $\mathcal{S}$  generated from  $\mathcal{O}$  ( $\rightarrow$  Algorithm 2)
2: for all nodes  $N_i \in \mathcal{S}$  do
3:   spawn all objects in  $N_i$  in simulation
4:   plan approach  $T_1^\alpha$  and extract  $T_2^\alpha$  trajectory
5:   move simulated robot on  $T_1^\alpha$ 
6:   grasp active object  $\alpha$ 
7:   move simulated robot on  $T_2^\alpha$ 
8:   release active object  $\alpha$ 
9:   determine manipulation costs  $V_{w,i}$  ( $\rightarrow$  Section 3.1)
10: end for
11: for all leaf nodes  $N_j^{\text{leaf}} \in \mathcal{S}$  do
12:    $V_{w,j} \leftarrow$  summed-up costs of  $N_j^{\text{leaf}}$ 's parents
13:    $V_{w,\min} \leftarrow \min(V_{w,\min}, V_{w,j})$ 
14: end for
15: output: node  $N_j$  with lowest manipulation costs  $V_{w,\min}$ 
```

algorithm has been used previously in [41] on a related problem. In the example in Figure 6, the initial configuration is shown as the tree root, on the top, while further down the tree one object has been unloaded in each node. The images show the respective initial configuration for these nodes, before performing the manipulation step. While traversing the tree further down, unintended motion and high costs are caused for the  which falls off the  when the latter is manipulated. The leaves merely contain one remaining object which can directly be manipulated disregarding the scene physics since no passive objects are left.

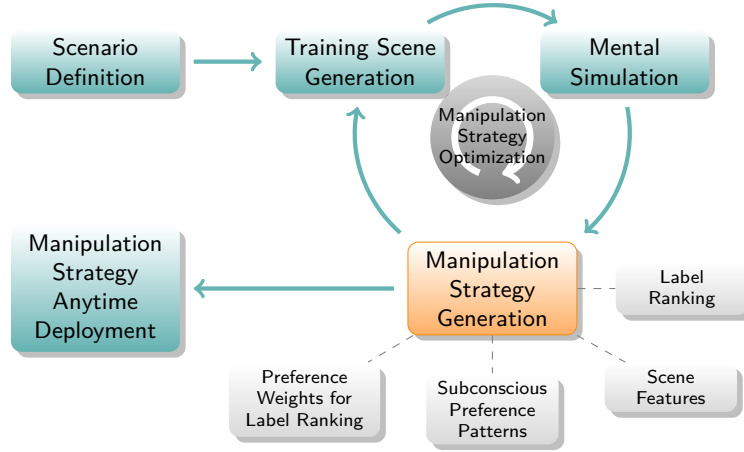
Algorithm 2 shows how to generate the search tree \mathcal{S} for a scene given the initial object configuration. This works in a recursive way, starting from the root node (level 0) which includes the initial configuration, down to the leaves where only one object is left in the scene. Each node $N_i \in \mathcal{S}$ contains the respectively assigned object set \mathcal{O}_i as seen in Figure 6, but not the poses of the objects. After the tree has been filled, traversing it works like shown in Algorithm 3, using a depth-first search-like technique, with the objective of finding the node with the minimum manipulation costs $V_{w,\min}$. During traversal, the final state of the mental simulation of each node is propagated into its child nodes. This determines the initial object poses for the respective child node prior to running mental simulation on it.

Using depth-first search may seem inefficient at first glance, however, in order to use A^* or a similar search algorithm for our problem we would need to design an admissible heuristic. Since damage avoidance is one of the main contributions of this publication, we use the Maximum Weighted Swept Convex

Volume V_w as a manipulation cost function which considers complex motion paths and changes of movement direction and spin. Both of these factors are a crucial ingredient to avoid objects toppling or dropping under all circumstances. However, it is not possible to define an admissible heuristic because the distance (in terms of our cost function) to the target configuration cannot be determined before actually having searched the tree till its leaves.

In Section 6 we will show the general feasibility and efficiency of our planning method. However, the whole mental simulation process may take extended time, especially for a growing number of scene objects. Therefore, the next section explains how to increase the overall efficiency by generating manipulation strategies which eventually replace time-consuming planning in the long run.

4 Manipulation strategy generation



One of the main contributions of the proposed approach is the *generation of manipulation strategies* from previously-planned manipulation sequences. Such a strategy comprises of a machine learning classifier which allows to *predict a sequence of manipulation actions* while applying some prior knowledge.

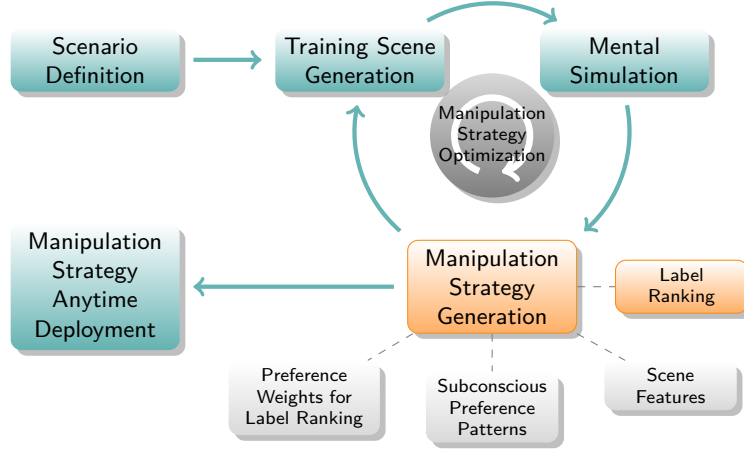
In our case, this prior knowledge consists of planned manipulation sequences on many different scenes where the prediction yields a desirable manipulation sequence for a new, previously unseen scene. All scenes can be characterized using certain distinct features; all features of a particular scene together with the anticipated optimal manipulation sequence form one training sample. *Label ranking*, a machine learning technique, then takes the part of predicting new manipulation sequences from the known training data given a set of scene features.

Learning-based approaches in a manipulation context exist in a large diversity of applications and used techniques, including learning the support order of piles and the geometric relations between objects therein [33, 39, 47] or object affordances [24]. However, manipulation strategy generation benefits from this only if it is able to take into account relational predicates like **in**, **on** and **behind** or support and containment relations. Additionally, assessing a scene for these predicates does not necessarily yield unambiguous results, especially for geometry-based predicates. Finally, since we want to take the surrounding

workspace into account as well, only describing relations between objects may not be sufficient for anticipating dynamic behaviors.

Another established field of research is grasp learning using different kinds of features and measures [10, 23]. This works in a similar way as our method with respect to the generation of a classifier which allows for predicting grasps for new situations, but on grasp level. Other learning-based approaches tackle problems like predicting physical effects on objects using visual features [31, 36]. However, none of these works deal with high-level sequencing which is the main contribution of our proposed method.

4.1 Label ranking using ranking by pairwise comparison



A label ranking classifier C basically solves the problem of *ordering a set of abstract labels \mathcal{L} with size $n = |\mathcal{L}|$ into a sequence $\pi \subseteq \mathcal{L}$* using a feature vector $\mathbf{x} \in \mathbf{X}$ such that $C : \mathbf{X} \rightarrow \mathcal{L}, \mathbf{x} \mapsto \pi$. The resulting sequence π is a permutation of all occurring labels where label $\pi(i)$ is ranked higher than label $\pi(j)$. Generally, this *pairwise preference of $\pi(i)$ over $\pi(j)$* is denoted as $\pi(i) \succ \pi(j)$.

In the literature, many different label ranking methods exist, based on different established machine learning algorithms. Amongst the most popular ones are Decision Tree-based [44, 7] and Gaussian Mixture Model-based methods [60, 15] as well as *ranking by pairwise comparison* (RPC) [19] which we use in the proposed approach.

RPC uses an ensemble of classifiers to predict pairwise preferences and afterwards employs a voting scheme to combine the atomic classifiers' outputs into a common prediction. Because of this, one important parameter of RPC is the way of how to combine classifier outputs into a prediction. There are two major voting schemes which have been evaluated for this purpose so far [18]: *binary voting* and *soft voting*. The former bases on the result of a binary classifier which emits whether or not the input corresponds with its learned preference. Soft voting, on the other hand, outputs a continuous value in $[0, 1]$ which can be interpreted as the confidence of the classifier about the compliance with the learned preference.

RPC proves advantageous for our purposes since the used atomic classifiers correspond to pairwise preferences which play a major role in our overall method. We will go into detail on this in Section 4.4 where pairwise preferences and

their importance in human-like intuitive manipulation is explained. One more major advantage of RPC in our use case is the fact that it qualifies as an *eager learning* method which uses a considerable amount of time for training the ensemble of classifiers, but prediction happens in near real-time. Since we defer the whole processing circle of training scene generation, mental simulation and manipulation strategy optimization (which includes classifier training) into load-free times, no delays are inflicted on productive use.

4.2 Distinction from related methods

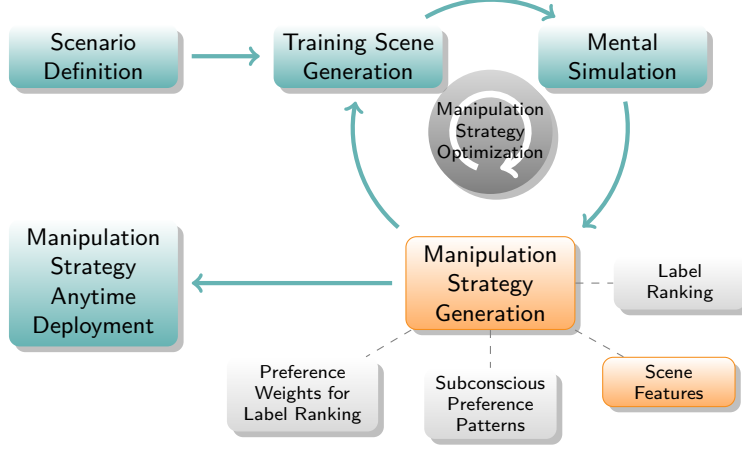
In contrary to label ranking, there are several methods which target problems overlapping with ours. However, these cannot be used in a similar way as our method, but are important to be isolated from it because they produce structurally and logically different results:

Structured prediction Instead of ranked labels, this method outputs binary flags which mark if a particular label is relevant to the input sample or not. This can be used to classify if an image falls into a category like "nature" or "architecture". Examples of packages using this technique are SVM^{struct} [20] and conditional random fields [51].

Learning to rank Although sounding similar in the first moment, this method provides solutions to a different problem, namely creating rankings of training samples and not rankings of abstract labels. One common usage is recording click-through preferences; the labels used as inputs into the algorithm are simply the sample indices in the training set. There is no possibility in this method to provide a ranking of abstract labels as training input. Prominent examples for learning to rank are RankNet [5] and ranking SVMs like SVM^{rank} [20, 21].

Sequence classification This term is usually used where only the sequences themselves, but no external training features exist, for instance when natural speech as a sequence of words is to be annotated with the respective word classes. Therefore this method only makes sense within context-rich environments where the exploitation of the latter satisfies the required generalization capabilities of some classifier. A survey of approaches using this technique can be found in [59].

4.3 Scene features



Ranking by pairwise comparison relies on atomic classifiers which base on multinomial logistic regression [19, 6]. These classifiers are used to predict a confidence for a pairwise preference $\pi(i) \succ \pi(j)$ from a given feature vector \mathbf{x} . Such features have to be descriptive for the respective scene in order to allow for reliable manipulation scene prediction in a new, unknown scene. In this subsection, we present the feature vector that is calculated from every training scene as an input to the manipulation strategy generation process.

4.3.1 Attentional vector sum

As a measure for semantic spatial relations between scene objects, we employ the *attentional vector sum* (AVS) model which is used in language comprehension research and was introduced by Regier and Carlson [42]. It has been extended in several refined models (e.g. by Kluth [27]) and used for similar problems in robotics (e.g. by Sjöö and Jensfelt [47]).

The AVS model generally evaluates spatial prepositions like **behind**, **above** and **left of** with respect to two distinct objects and provides an acceptability rating for the respective predicate in the shape of

$$\text{above}(\text{object1}, \text{object2}) = 0.1 \text{ where } \text{above}(\cdot) \in [0, 1].$$

In our application, we evaluate the AVS for each of the prepositions **in front of**, **behind**, **above**, **below**, **left of** and **right of** from the robot's point of view for each permutation of two objects.

4.3.2 Visibility

Another important feature of a scene with respect to the manipulation order is object visibility which intuitively correlates with the manipulation difficulty level. Hence, we compute the visibility ratios r_{vis} of all objects $o \in \mathcal{O}$ as follows:

$$r_{\text{vis}}(o) = \frac{V(H(\mathcal{C}(o)))}{V(H(\mathcal{M}(o)))} \quad (4.1)$$

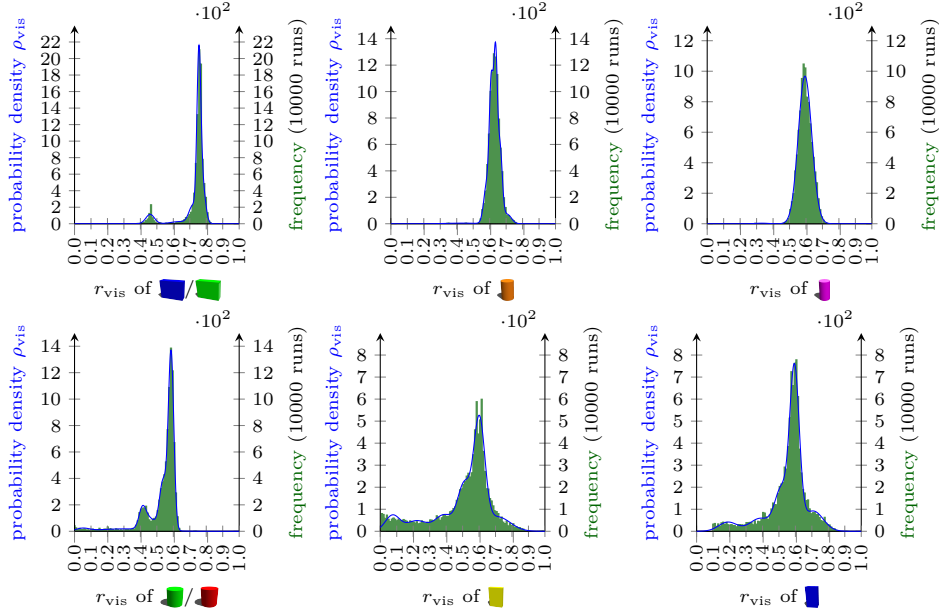




Figure 7: Gaussian mixture model probability densities ρ_{vis} for visibility ratios r_{vis} of different objects in the logistics (top) and supermarket (bottom) scenarios

where $\mathcal{C}(o)$ is the 2.5-D point cloud of o visible in the scene, $\mathcal{M}(o)$ is o 's previously known 3-D object model, $H(\cdot)$ denotes a convex hull and $V(\cdot)$ the volume of such a hull.

In order to abstract from object-dependent probability distributions for the visibility ratio which result from self-occlusion, we first generate 10000 scenes per object with the object randomly placed and rotated in the workspace of the respective scenario. Afterwards, we fit a *Gaussian mixture model* (GMM) on the **histograms of frequencies** of visibility ratios r_{vis} occurring in each run (see Figure 7). The number of GMM components as well as the covariance type were optimized by minimizing the Bayesian Information Criterion [45].

The **probability density ρ_{vis}** of the GMM then is taken as the final visibility score which is still an object-specific value, but generalizes away from multi-modal distributions of the visibility ratios r_{vis} like for  and  as can be seen in Figure 7.

Note that the visibility scores of the objects in the Supermarket scenario (Fig. 7 bottom row) are less distinct than the objects of the Logistics scenario (Fig. 7 top row). This is caused by the high-altitude camera position which requires a strong tilt in order to have the whole shelf in view. Hence, the sensor data on the margins of the field of view may sometimes be cropped, causing objects' visibility ratios to drop when randomly spawned close to the shelf margins. Please also note that r_{vis} usually does not take values close to 0 because some part of the object is always visible, otherwise it would not have been recognized by the perception system. Additionally, r_{vis} values close to 1 do not occur because the 2.5-D input point clouds are subject to self-occlusion, hence the back part of the objects is cropped.

4.3.3 Feature vector

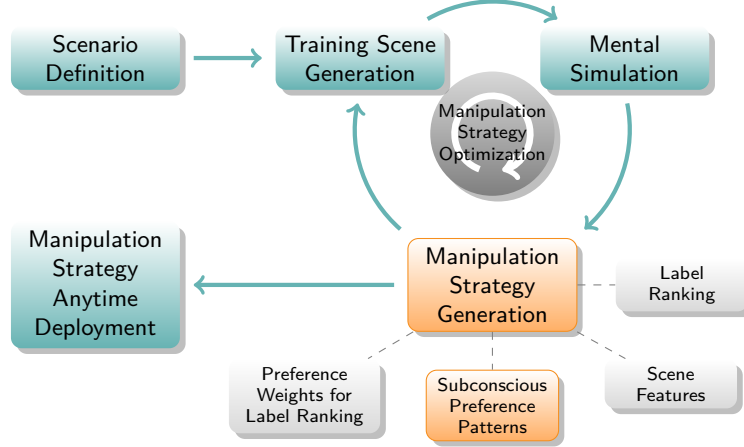
In addition to the more complex AVS and visibility features, we compute several object-specific and object-relational features as shown in Table 1.

The final set consists of $23n + 17p$ features with the number of objects in the scene being $n = |\mathcal{O}|$ and the number of all possible object pair combinations being $p = \binom{n}{2}$. For a scene comprising four objects, this would end up in a 194-dimensional feature vector \mathbf{x} . One concrete instance of \mathbf{x} , together with the respective manipulation sequence π as determined from mental simulation, eventually forms one training sample for C with $\mathbf{x} \mapsto \pi$.

Feature (object-specific)	Dimensionality
Pose within the scene	$6n$
Distance vector to workspace bottom	$3n$
Distance vector to workspace back	$3n$
Distance vector to initial gripper position	$3n$
Visibility ρ_{vis}	n
Axis-aligned bounding box size	$3n$
Oriented bounding box size	$3n$
Free space around object (= Euclidean distance to closest object's surface)	n
Feature (object-relational)	Dimensionality
Distance vector per object pair	$3p$
Euclidean distance per object pair	p
Contacts per object pair (point, normal and force)	$7p$
AVS for 6 prepositions per object pair	$6p$
Total	$23n + 17p$

Table 1: Features and dimensions, number of objects $n = |\mathcal{O}|$, number of object pair combinations $p = \binom{n}{2}$

4.4 Subconscious preference patterns



Whenever a human needs to decide between two alternatives like "Should I take A or B?", they use some inherent classification scheme from their prior knowledge to come up with a decision. In a situation that requires motoric interaction on two objects, the decision which one to manipulate is driven by the concrete scene and objects, but also by physical properties of the human itself.

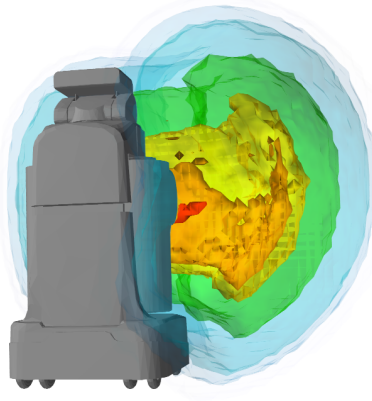


Figure 8: Kinematic reachability of the PR2’s right arm
 image adapted from http://openrave.org/docs/0.6.6/_images/tutorial_inversereachability_back.png
 © 2006-2017 OpenRAVE, available under the the Creative Commons Attribution 3.0 license

Imagine, for instance, a right-handed user who, whenever possible with respect to occlusions, reachable workspace and other kinetic limitations, always grasps with their right hand. For a setting where two objects are similarly reachable, but one needs to be grasped with the right and the other one with the left hand, a right-handed human, minimizing physical effort, would naturally know which one to grasp best.

Now imagine a scenario with a robot for which grasping object A is easier than grasping object B in a specific scene because of

- limited workspace due to manipulator size, position on the robot base and number of degrees of freedom
- scene obstacles preventing from reaching object B
- uneven probability distributions in the stochastic motion planner which make it more likely to obtain solutions for object A
- the grasping pose of object B, which is sampled from the noisy object representation, being located outside of the manipulator workspace.

One good example for such a scenario is the PR2 robot in the supermarket (Fig. 2b) which we, for the ease of obtaining viable grasping configurations, use in a right handed-only way, i.e. the left arm is tucked up while grasping only with the right one. Consequently, a tendency to grasp objects on the right first can be observed in scenarios using this robot configuration – see the robot arm’s kinematic reachability in Fig. 8.

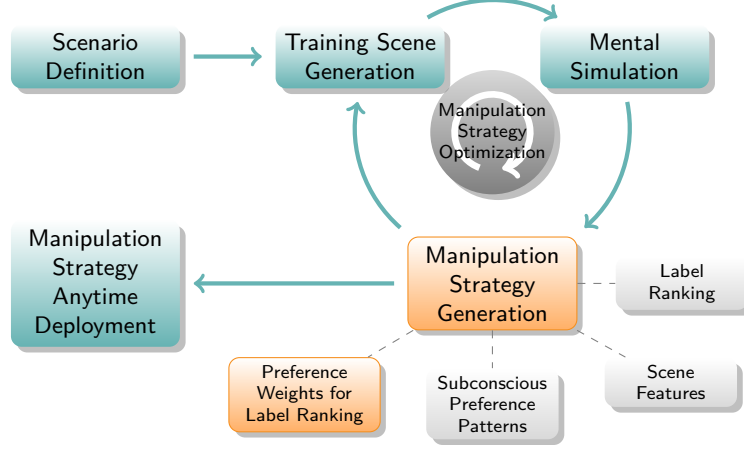
Therefore, noise on object pose and grasping pose level plays an important role when considering which object to prefer for grasping. Many publications deal with circumventing such noise and finding manipulation plans nevertheless, e.g. [3, 54, 34, 56], amongst many others.

However, humans deal with such noise intuitively, implicitly taking into account all mentioned constraints. Over many observations, *subconscious preference patterns* become apparent as we show in our experiments. Our approach

integrates these patterns in a way that, as for determining a manipulation sequence for an unknown scene, the robot behaves humanlike in a way that certain manipulation actions are more likely than others for the reasons stated above. Since many underlying sources are encoded into the presented method’s output, changing properties like the used motion planner or the robot model will get reflected in the manipulation sequence predictions similar to human long-term knowledge.

In our evaluation (see Section 6) we show how such preference patterns emerge from our considered application scenarios. As described above, we use *ranking by pairwise comparison* as a label ranking method which is particularly useful because it employs the mentioned preference patterns to create a classifier which can derive a ranking. The next subsection describes how we apply this method in the course of our overall approach.

4.5 Preference-weighted label ranking



Using the preference patterns as described above and the feature vector \mathbf{x} , the original *ranking by pairwise comparison* (RPC) method combines them into a final ranking by calculating the sum of votes like described in [19]:

$$s = \sum_{\pi(i) \succ \pi(j)} C_{ij} \quad (4.2)$$

where $C_{ij} : \mathbf{X} \rightarrow \mathcal{L}, \mathbf{x} \mapsto \pi$ is the output of the base classifier for $\pi(i) \succ \pi(j)$ and n labels. In case of using *soft voting* (see Section 4), $C_{ij} \in [0, 1]$, whereas for *binary voting* $C_{ij} \in \{0, 1\}$, i.e. the input does or does not belong to the respective class.

Since it is our goal to regard the label ranking process from a preference-pattern viewpoint, the following enhancement allows for taking into account *preference weights* w_{ij} when computing the sum of votes:

$$s = \sum_{\pi(i) \succ \pi(j)} v_{ij} \quad (4.3)$$

where

$$v_{ij} = \begin{cases} w_{ij} \cdot C_{ij} & \text{if } C_{ij} > 0.5, \\ 0 & \text{otherwise,} \end{cases} \quad (4.4)$$

$$w_{ij} = \frac{|\{(i, j) \mid \pi(i) \succ \pi(j)\}|}{m}, \quad (4.5)$$

and m is the number of training samples.

The weights w_{ij} are used to balance a certain preference $\pi(i) \succ \pi(j)$ versus its inverse $\pi(j) \succ \pi(i)$. Given our training data with 100 samples per scene to minimize the influence of noise in the physics simulation and motion planner, they are formed by the proportion of a particular preference in relation to the whole training data. This way, the resulting ratio indicates how likely a particular object will be preferred over another in this particular scene configuration.

In the practical process of generating manipulation strategies, we now train a classifier using the described preconditions and additions to RPC. The resulting classifier, spawned from the training data which was extracted from auto-generated scenes, forms the current *manipulation strategy* of the robot in the given environment. This strategy can be optimized in a simulation-in-the-loop cycle as we will explain in detail in Section 5.

However, our experimental evaluation shows that the integration of preference weights into the classifier training process did not show a significant increase in prediction fidelity for our use cases compared to the original RPC method (see Section 6.2.5). Nevertheless, we use the preference weights to meaningfully compare two manipulation strategies. In order to do this, a loss function $l(\pi, \pi')$ which gives the difference between two rankings π and π' has to be defined. In our approach we count the number of pairwise preferences appearing in inverse order (*discordant preferences*) compared to the training data, i.e.

$$l(\pi, \pi') = |\{(i, j) \mid \pi(i) \prec \pi(j) \wedge \pi'(i) \succ \pi'(j)\}|. \quad (4.6)$$

Since, for evaluation of the presented method, we additionally need a similarity measure in order to make sound statements about the resulting rankings, we use the established *Kendall rank correlation coefficient* [25], commonly denoted as *Kendall's tau coefficient* $\tau : \mathcal{L} \times \mathcal{L} \rightarrow \mathbb{Q}, (\pi, \pi') \mapsto \tau$ with

$$\tau(\pi, \pi') = 1 - \frac{4l(\pi, \pi')}{n(n-1)} \quad (4.7)$$

where $n = |\mathcal{L}|$ is the number of labels to appear in the ranking. In the use case of manipulation sequences, this equals with the number of objects in the scene.

As a side note, in the context of label ranking, many approaches use some form of weights to allow for adaptation of their algorithms to the respective domain. Nevertheless, the definition of these weights usually does not match the preference weights defined above, like in [46] where the authors assign per-label relevance weights different in every sample. The same applies for the labelwise weight variant of τ in Kumar and Vassilvitskii's work [28] which only depend on the label itself, but not on its relation to other labels.

Since we have the necessity for preference weights which consider a pairwise permutation of labels, though, we propose the *preference-weighted Kendall's tau* rank correlation measure $\tau_w : \mathcal{L} \times \mathcal{L} \rightarrow \mathbb{R}, (\pi, \pi') \mapsto \tau_w$ with

$$\tau_w(\pi, \pi') = 1 - \frac{4l_w(\pi, \pi')}{n(n-1)}, \quad (4.8)$$

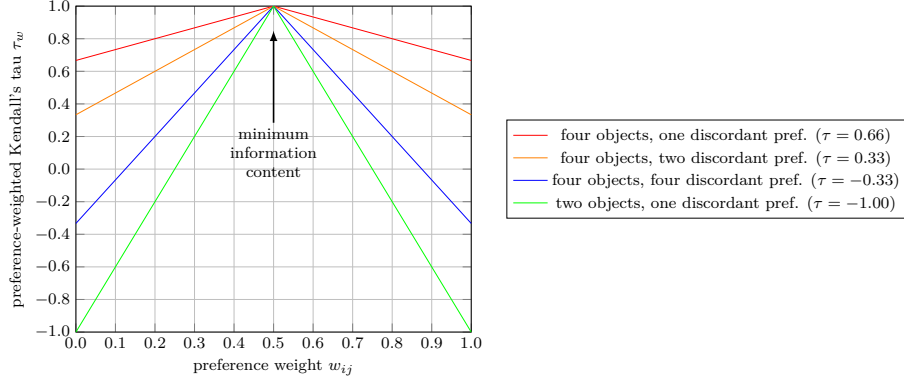


Figure 9: Preference-weighted Kendall’s tau τ_w relative to preference weights w_{ij} w.r.t. different numbers of discordant preferences and objects

$$l_w(\pi, \pi') = \sum_{\pi(i) \succ \pi(j)} d_{ij}, \quad (4.9)$$

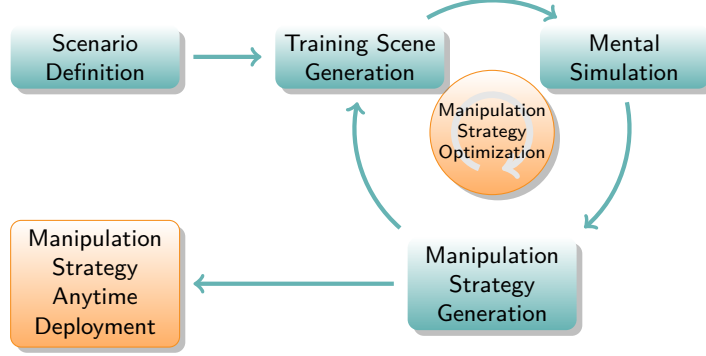
$$d_{ij} = \begin{cases} \max(w_{ij}, w_{ji}) - 0.5 & \text{if } \pi(i) \prec \pi(j) \wedge \pi'(i) \succ \pi'(j) \\ 0 & \text{otherwise} \end{cases} \quad (4.10)$$

where w_{ij} is the preference weight of the respective pairwise preference $\pi(i) \succ \pi(j)$ computed from the noisy training data of one scene as in Eq. 4.5 and $n = |\mathcal{L}|$ is the number of labels to appear in the ranking.

This way, wherever the distance between two rankings is to be calculated using τ_w , every preference that appears only in one of the rankings gets weighted with the respective preference weight. Figure 9 shows an example of τ_w scaling between 1.0 and the respective τ when the weights scale between 0.5 (completely random, no preference, minimum information content) and 1.0 (strong preference, maximum information content). The resulting τ_w allows for continuous values with an image cardinality of $|\tau_w[\pi, \pi']| = |\mathbb{R}|$ as opposed to τ which has a discrete image with a cardinality of only $|\tau[\pi, \pi']| = 2n - 1$ for n labels. This bears the advantage that the more fine-grain τ_w can distinguish pairs of sequences according to preference relations where the coarse-grain τ provides the same measure for these pairs. In the evaluation section, we will show examples why and how this is useful for our method.

Summarized, in this section we described how to generate manipulation strategies from mentally simulated manipulation sequences. These can now be deployed in a real application scenario and continuously optimized as described in the following.

5 Wrapping everything up: Self-supervised free-time manipulation strategy optimization for anytime deployment



Having defined our full procedure of auto-generating training scenes and extracting the respective training data, we are now able to generate manipulation strategies using our Ranking by Pairwise Comparison classifier and optimize them in a self-supervised manner. This happens during load-free times of the robot which typically occur during night hours or weekends or even, guarded by a task scheduler, during regular operation while the current CPU load permits.

Algorithm 4 Self-supervised manipulation strategy optimization

```

1: generate initial set of training scenes4
2: extract samples from training scenes using mental simulation
3: add new samples to training and testing set with a 2:1 ratio
4: while CPU load low and not interrupted do in several Docker containers in parallel
5:   while not interrupted do in parallel
6:     update classifier
7:     - retrain classifier with new training set
8:     - evaluate classifier on testing set, discard new samples if  $\tau_w$  decreased
9:   generate more training samples
10:  - generate training scenes
11:  - extract samples from training scenes using mental simulation
12:  - add new samples to training and testing set with a 2:1 ratio
13:  end while
14: end while
15: deploy classifier anytime to predict a manipulation sequence for a real scene
  
```

Algorithm 4 describes the individual steps of the strategy optimization cycle. Depending on the free computing capacities on the robot, one iteration of this loop varies in runtime, hence the per-time utility improvement of the respective classifier is subject to other tasks being executed at the same time. Therefore a manipulation strategy may take a long time to converge⁵ if not operated during load-free runtimes. The prediction of manipulation sequences on real scenes, however, happens instantly in near-real time with the currently built classifier. Our method can be classified as an *anytime algorithm* because it always delivers a valid result, even when interrupted, and improves upon its solutions the longer

⁴The initial training set size should depend on the maximum tolerable time until the classifier is required for the first time.

⁵Convergence of our optimization method strongly depends on the concrete implementation and application scenario and is hard to define generically as we will explain in the evaluation.

it keeps running.

In the next section we show how, through multiple strategy optimization cycles, the overall prediction accuracy increases and the manipulation strategy adheres more and more to the discovered preference patterns. Nevertheless, if the user decides to accept the currently active strategy for deployment, they can do so anytime. However, as soon as the next load-free time slot appears, the manipulation strategy optimization cycle can be continued where it was interrupted. As for bootstrapping our method on a newly deployed robot, the latter initially incorporates no knowledge about manipulation strategies, but the environment and object models have to be known beforehand. Our method does not put any semantic constraints on the objects or the combinations into which they are grouped to train an individual classifier. Hence, the order of object combinations to be learned can be purely application-driven, e.g. commencing with classifiers for combinations of low numbers of objects in order to quickly converge towards viable classifier performance. Later during robot lifetime, training of larger combinations can be performed which is more computationally intensive, but the robot can meanwhile continue working with the classifiers trained up to that point.

One major advantage of the proposed self-supervised strategy optimization method is that it allows for effortless parallelization. Our experiments were performed using a setup of multiple similar *Docker*⁶ [32] containers executed in parallel, increasing the overall system efficiency even more. Additionally, the generation of training samples can run in parallel to updating the classifier with the existing set of samples, so this increases the system efficiency even more. We provide a generic version of our parallelized container setup⁷ together with some usage examples and Gazebo models, partly created using our previous work [12].

Summarized, our *simulation-in-the-loop* approach allows for continuous self-supervised optimization of the current manipulation strategy, leading to more accurate predictions with respect to reality over robot lifetime.

6 Evaluation

In order to evaluate our approach, the coherency with respect to human behavior as well as efficient strategy optimization cycles play an important role. In this section, we will estimate the worst-case complexity of different parts of our approach and explain which measures were taken to improve the overall efficiency. Afterwards, several experiments on different application scenarios show the performance of the presented method within the specific steps and, finally, the performance of the full self-supervised strategy optimization cycle.

6.1 Efficiency considerations

6.1.1 Training data generation

In Section 4.5 we described an idea of how to integrate preference weights w_{ij} into the RPC classifier. However, as shown in our experiments (Section 6.2),

⁶<https://www.docker.com/>

⁷<https://github.com/jacobs-robotics/gazebo-mental-simulation>

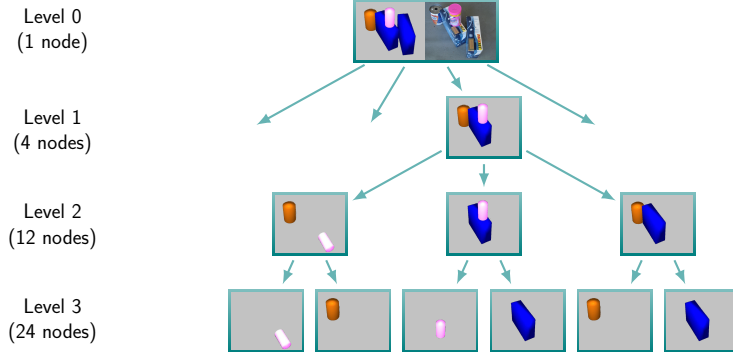


Figure 10: Example search tree

Some branches cropped for increased visibility. Each node shows its initial configuration, i.e. prior to manipulation. Recap of Fig. 6.

the weights do not significantly improve the performance of the classifier if integrated into the prediction process. Nevertheless, we use the preference weights to calculate τ_w as a performance measure for our evaluation.

On the other hand, this means that the manipulation strategy generation part of our method experiences a speedup of 100 with respect to integrating the preference weights into classifier training because they do not need to be calculated during self-supervised fully-autonomous operation. Hence, it is not necessary to plan manipulation sequences for a specific scene more than once.

6.1.2 Planning efficiency

In contrast to A^* or other common search methods like discretized Rapidly-Exploring Random Trees (RRT) or Rapidly-Exploring Random Leafy Trees (RRLT) [35], our scenario causes an efficiency issue in estimating the node costs and not in the search itself. Traversing the tree taken by itself is rather trivial and fast because the number of nodes which are handled in our search trees can be processed rapidly on modern machines. Thus, the efficient search problem is overshadowed by a heuristic cost estimation problem during the processing of each individual node which is prominent and crucial to solve in minimal time.

The *worst-case* tree size for a number of objects n , constructed from all possible permutations of the object set like in Algorithm 2, is

$$\sum_{i=0}^n \frac{n!}{(n-i)!} = 1 + \frac{n!}{(n-1)!} + \dots + \frac{n!}{2} + n! \quad (6.1)$$

where $\frac{n!}{(n-i)!}$ is the number of objects for the respective tree level i , $i = 0$ representing the top level (i.e. root), $i = n$ the bottom level (i.e. leaves); see the example in Figure 10. However, our experiments in the next subsection show that this number is never reached in practice due to different possibilities of pruning the tree during planning.

6.1.3 Scene clustering

Equation 6.1 showed a nonlinear increase in search tree size with a rising number of scene objects, taking along the cost estimation problem with the same speed. As a remedy, we suggest to break down scenes with many objects into smaller clusters of $n \leq 4$ objects which are then treated individually. Practically, as regarded in Section 4.4, the robot will anyway not be able to physically access more than a low number of objects from a certain point of view due to space and dexterity constraints. However, the exact way of clustering scene objects strongly depends on the scenario and a generic consideration of this subproblem does not fit the scope of this publication and has to be treated in future work. Most importantly, however, is the fact that during deployment of a trained classifier in a productive setting the per-cluster application of an individual classifier instead of one single classifier for the whole scene creates no tangible efficiency loss since the prediction runtimes of RPC lie in the sub-second range.

In any case, using smaller object clusters mitigates the issue that the reachability of scene objects strongly depends on the robot kinematics and hence often is limited by a large extent. In the course of complex manipulation procedures like used in our approach, the higher the number of objects in a cluttered scene grows, the less likely any valid grasping configurations can be generated for each individual object. To stay with the PR2 supermarket example, a right-handed robot may have severe difficulties manipulating objects on its left-hand side. In this case it is reasonable to handle clusters to the left of the robot with lower priority if only the right arm is used for manipulation. Nevertheless, even when only using a part of the scene as active objects, the remaining objects should still be included in the simulated scene. This way, if any passive object is moved accidentally, even if it is not active anywhere in the search tree, it will still account for the cost function.

6.1.4 Search tree optimization

In addition to not using more than a certain number of objects at a time, we cut off as many branches of the search tree as possible in which ultimately there is no possibility to present the optimal solution. In the following, we will present several ideas to reduce the tree size as far as possible. In Section 6.2 we show that the tree size in a typical scenario can be reduced to as low as 48.7% using these measures.

Implicit search tree pruning: As we show by an empiric consideration in the Experiments section, in every scene there is a number of configurations which implicitly cannot be simulated. Usual reasons for this are that approaching an object may push a passive object which, in turn, moves the active object away by a significant distance. In this case, the active object will end up unreachable for the planned manipulation action. Additionally, sometimes no feasible grasping configuration can be found without the robot colliding with the environment (container, shelf, etc.). Since motion planning is out of scope of our work, we have to skip simulating the respective configuration in this case and impose infinite costs.

Explicit search tree pruning: In addition to the implicit reasons given above, the used depth-first search allows for cropping tree branches: After simulating a configuration, if the accumulated costs in the current branch exceed the total costs of any already computed goal sequence (i.e. a tree leaf), we stop exploring the current branch.

Reuse of similar configurations: Another way to reduce computational load, in addition to pruning tree branches, is to reuse similar configurations which occurred before somewhere else in the tree. Before running the simulation, we compare the current configuration to each one which was simulated before, anywhere in the tree, for similarity of objects and their poses. If there is a similar configuration, we reuse this node and the whole child tree of the node (if any) without having to simulate any of them. This idea has already been described as efficient by Peshkin and Sanerson [41].

Generally speaking, apart from the mentioned measures to reduce computational complexity, the runtimes of our method strongly depend on the used simulator. Moreover, regarding the total runtime of one mental simulation run, motion planning and execution take the biggest part of time which is very robot and application-specific.

Fortunately, our method is well-suited for parallelization because all nodes on the same tree level can be simulated in parallel since their configurations do not depend on each other. As the number of objects in the scene and, with it, the number of tree levels rises, the limit for the speedup achieved by parallelization is the number of used threads / CPU cores.

6.2 Experiments

In order to evaluate our method with respect to real-life usage, it is important to note that no ground truth exists other than human intuition which our results can be compared with. The only way of providing ground truth manipulation sequences is human assessment with the human built-in mental simulation capabilities being prone to abstracting and simplifying complex dynamics just as a physics engine. Hence, the following results have to be judged using common-sense intuition since we are not aware of any comparable approaches presented so far which would provide a baseline dataset.

6.2.1 Application scenarios

We want to evaluate our method applied on two of the described practical scenarios, typical scenes of which are shown in Figure 11. As for the first scenario, logistics is a field where many different goods have to be handled, some of which are heavy, bulky, fragile or otherwise damage-prone. Our previous work on unloading shipping containers [49] provides an ideal application in this respect, so we have modeled the robot, container and objects from this scenario as our first example. Secondly, domestic and retail robotics provide another playground for mental simulation, thus the supermarket scenario of [58] will serve as the second example.

Logistics Scenes 1 and 2 in Figure 12 show typical logistics scenarios where scene 2 is the most challenging one due to the goods supporting each other.

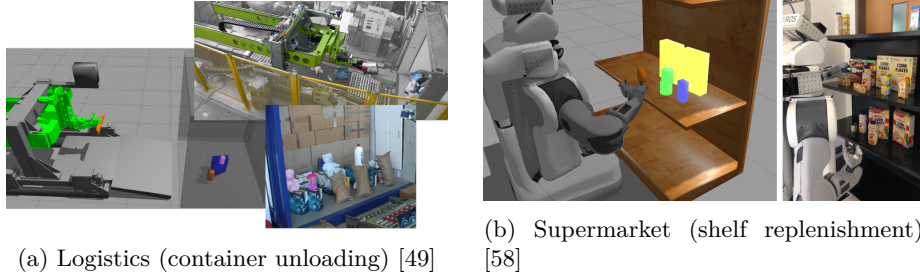




Figure 11: Application scenarios for autonomous manipulation [11] (recap of Fig. 2)

Hence, once any of the objects is manipulated it is likely that one of the others will move as well.

Supermarket The tall shelf in scenes 3 and 4 (Figure 13), along with the cans which may roll away if dropped, is a hostile area for any damage-prone product and thus a good example for our method. The tipped-over items in scene 4 occur frequently in a supermarket where customers leave the shelf like this, products coming to rest partly on top of each other.

6.2.2 Mental simulation

We ran our mental simulation (Algorithm 3) 100 times each on the two exemplary scenes per application.

The left column of Figures 12 and 13 shows how often a particular manipulation sequence π was selected. A clear preference for a specific sequence is visible for all of the scenes, however, in Scene 3, the distance in frequency between the first and second-ranked sequence is less distinct. This stems from the fact that, in the given object configuration, it does not seem to make a big difference regarding possible damage whether, for instance, the  or the  is manipulated first. In the other scenes, however, the objects bear a higher spatial dependency on each other and it is more likely to distort the setup when manipulation them in any other than the top-ranked order. Summarized, these results show that mental simulation within the presented method is effective per se on different object and robot configurations.

Regarding the efficiency of the proposed approach, several generic means of optimization have been explained in Section 6.1. With respect to these, the following concrete criteria have been evaluated in the numerical results shown in Table 2:

- *mean first-ranked costs per node*: mean over all planning repetitions of the mean costs per object imposed on the manipulation sequence selected by Algorithm 3
- *mean second-ranked costs per node*: mean over all planning repetitions of the mean costs per object imposed on the second-ranked manipulation sequence

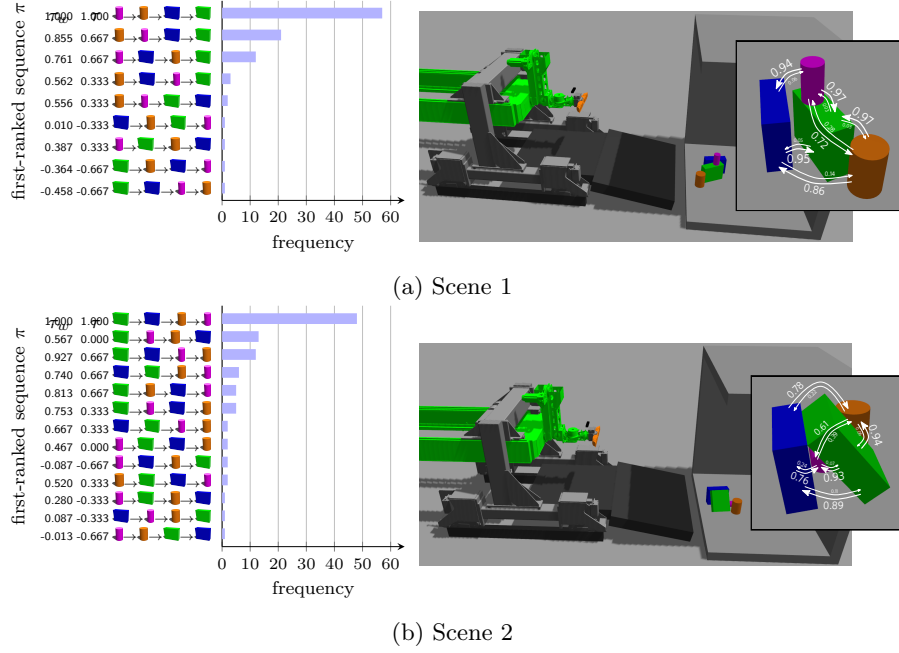


Figure 12: *Logistics scenario*: frequencies of first-ranked sequences π (center), τ_w and τ with respect to the first-ranked sequence (left) and preference weights w_{ij} for pairwise preferences (right) from 100 planning repetitions per scene

- *pruned tree nodes*: percentage of nodes pruned from the tree, resulting in a similar reduction in runtime, and composed of the following sub-criteria:
 - *known subtree*: a node shares its object configuration and poses with a previously processed node, thus the costs were copied without re-simulating
 - *costs exceed existing sequence*: a solution is existing already which has lower costs than the costs accumulated so far in this branch
 - *active object moved*: the active object was pushed away during approach, ending up unreachable
 - *object out of workspace*: an object fell out of the workspace (container/shelf), causing maximum damage and ending up unreachable for the robot
 - *planning failure*: no motion plan was found for the active object, e.g. because it was pushed away too far in a parent node
- *nodes with significant movement*: percentage of nodes which were not pruned from the tree and reported significant costs above a manually defined threshold

Table 2 shows that pruning the tree is generally effective, eliminating a mean of 51.3 % of nodes from the tree during the planning process. Since the planning time behaves linear with respect to the number of nodes to cover, this means

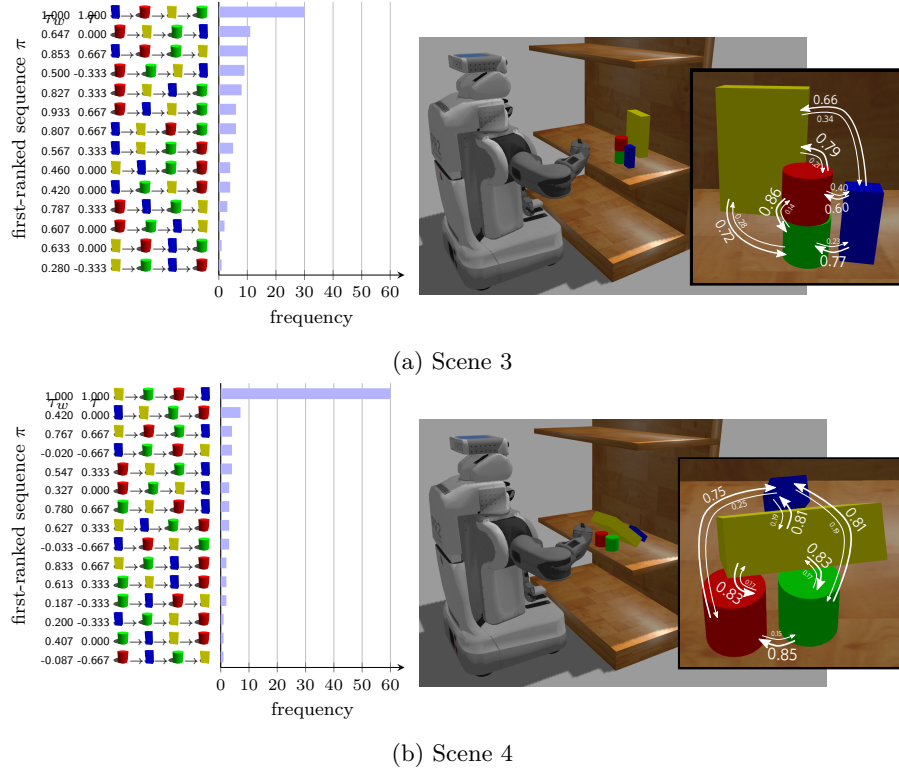

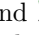

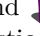
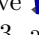
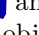
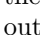
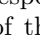




Figure 13: *Supermarket scenario*: frequencies of first-ranked sequences π (center), τ_w and τ with respect to the first-ranked sequence (left) and preference weights w_{ij} for pairwise preferences (right) from 100 planning repetitions per scene

Scene	1	2	3	4	Total
costs per node					
- first-ranked sequence	1.008 \pm 0.008	1.208 \pm 0.074	1.349 \pm 0.359	1.975 \pm 0.321	1.382 \pm 0.435
- second-ranked sequence	1.337 \pm 0.868	1.429 \pm 0.326	1.700 \pm 1.728	3.764 \pm 7.393	2.051 \pm 3.878
pruned tree nodes					
- known subtree	7.5% +	2.6% +	1.2% +	0.0% +	2.8% +
- costs exceed existing seq.	16.5% +	18.3% +	19.3% +	41.0% +	23.8% +
- active object moved	5.8% +	25.2% +	4.2% +	8.1% +	10.9% +
- object out of workspace	0.0% +	0.0% +	31.9% +	7.0% +	9.6% +
- planning failure	5.0% +	4.3% +	1.7% +	5.8% +	4.2% +
nodes with significant movement (costs > 2.0)	13.8% +	11.9% +	14.8% +	18.9% +	14.9% +


Table 2: Mental simulation numerical results: means and standard deviations of 100 planning repetitions

that one planning run can be completed in average within less than half the time compared to using an unpruned tree.

In Scene 2, a high number of nodes had to be skipped because the active object moved during approach. This is caused by the  and  hiding the  and  from the robot’s view. Therefore, our approach which is collision-agnostic with respect to passive objects made the passive  and/or  push the respectively active  or  away. Regarding Scene 3, an object has moved out of the workspace in 31.9% of nodes. This was caused by the round  which, when the  is extracted from underneath, often rolls away and falls off the shelf.



Nevertheless, such exceptional cases can be caught and a feasible sequence can be found by our method. In total, although in many cases the computed manipulation trajectories did not cause significant disturbance in the scene, in 14.9% of nodes significant movement was detected which, in real-world execution, may have led to non-negligible damage. Within tree search, however, these nodes have generally been avoided as shown in the first-ranked per-node costs. These are low enough to ensure the provided manipulation sequences are damage-minimizing.

6.2.3 Subconscious preference patterns

When looking at the initial scene configurations, most of the selected sequences in the left column of Figures 12 and 13 intuitively make sense, however, certain preferences in a single run may look counter-intuitive. One example for this is the  which surprisingly often turns up as a non-preferred object. This particular case can be explained with the fact that the robot has to extend its manipulator quite far to grasp this object, hence pushing other objects off the shelf if they are still present.

Nevertheless, such preference patterns may evolve from many repetitions on the same scene unexpectedly, depending on the object constellation, robot location and other factors. The images on the right of Figures 12 and 13 show the respective preference weights w_{ij} for the pairwise preferences of each object over all others.

The results show that, consistent with human intuition, generally objects whose centroid is higher than the one of other objects or which are resting on other objects are preferred. Other than that, objects obstructing a direct manipulation trajectory between gripper and objects in the back will be manipulated first in the most cases. In scenes 3 and 4, where the PR2 was used, there is an additional clear preference of objects which are situated at the right of other objects. This is not surprising since the right arm of the PR2 was used for manipulation, hence granting a bigger workspace to the right side as can be seen in Fig. 8.






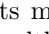
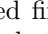

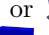

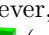

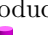

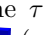
Several other preferences, like between the  and  in scene 3, however, are less expressive in the way that the preference weights lie close to 0.5. This implies a minimum of information content because each direction of the preference is equally likely. This phenomenon is caused by the fact that a large number of viable grasping configurations can be generated easily for these objects in this configuration given the robot workspace and dexterity.

Summarized, even though it is very difficult to denote preferences patterns as encountered in our experiments manually in an extensive way, our method is

capable of discovering them.

6.2.4 Preference-weighted Kendall’s tau τ_w

In the next subsection, we will show the behavior of our classifier for different settings with the help of the exposed preference patterns during classifier training and prediction. The preferences are embedded into the τ_w measure which gives very distinct results for sequences with identical τ . This results in an improved utility of the continuous τ_w as opposed to τ which gives coarse discrete values, as can be seen in Figures 12 and 13.

An example for this is the sequence  \rightarrow  \rightarrow  \rightarrow  ($\tau_w = 0.387$) in Fig. 12a where  gets moved first is obviously prone to accidentally moving  or . However, although they all produce the same τ of 0.333, in  \rightarrow  \rightarrow  \rightarrow  ($\tau_w = 0.562$) and  \rightarrow  \rightarrow  \rightarrow  ($\tau_w = 0.556$) it is less likely that a passive object is pushed away. Hence, in contrary to using τ as a suitability measure, these sequences are better distinguishable using their τ_w measure which takes the pairwise preferences into account.

6.2.5 Ranking by pairwise comparison

In order to show the performance of our overall classifier, we generated a series of 80 training scenes with five variants each which carry stochastic object pose noise. For each scene variant we collected 100 samples of manipulation sequences by running our mental simulation method on them in order to account for noise in the simulation itself, like described in Section 6.2.2. In total, this amounts to $80 \cdot 5 \cdot 100 = 40000$ samples, each containing a feature vector and the manipulation sequence determined using our planning method.

This data set was fed into classifier training in different configurations of the voting method and with/without integrating preference weights. Every run, the classifier was trained with a random 2:1 training/testing split on the respectively indicated number of scenes and evaluated on the testing split afterwards. 100-fold repetition of this training/testing loop yielded the distributions of results shown in Fig. 14.

As we will show in more detail in the next subsection, the results generally improve with the number of scenes. However, Fig. 14 shows a difference in performance for many of the considered configurations, especially regarding the variance of the distributions. Generally, it is more desirable to obtain low-variance distributions rather than high-variance ones with a similar median because the former mean higher precision and hence show to be more resilient against noise. Nevertheless, any bias in the distribution harms the precision, but positive bias w.r.t. τ_w means an increase in accuracy. Therefore, gauging accuracy versus precision of our results is important for the overall assessment.

Concretely, even though our results show no significant difference between configurations with our without injected preference weights, the weights themselves cohere with intuitive behavior. Hence we enable a deeper understanding of the classification results by providing the τ_w metric which allows for measuring this coherency. Without this τ_w metric which incorporates the preference weights, we would not be able to show that the learned manipulation strategy adheres to the subconscious preference patterns discovered using our method.

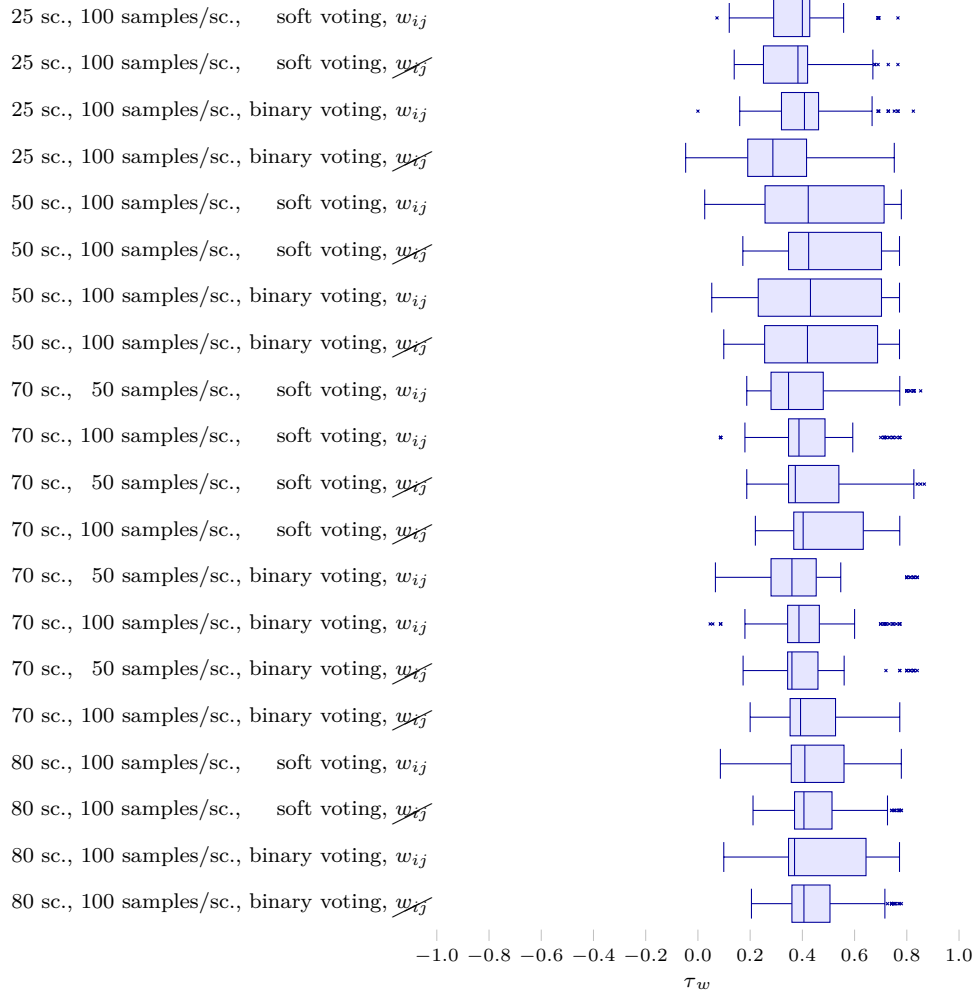


Figure 14: Results for manipulation strategy generation: τ_w for different numbers of scenes and samples per scene, binary/soft voting, with/without preference weights, each scene sampled five times with stochastic object pose noise.

Median, lower and upper quartile (Q_1/Q_3) over 100 classifier training repetitions. Lower and upper fences were calculated using $Q_1 - 1.5 \cdot (Q_3 - Q_1)$ and $Q_3 + 1.5 \cdot (Q_3 - Q_1)$, respectively.

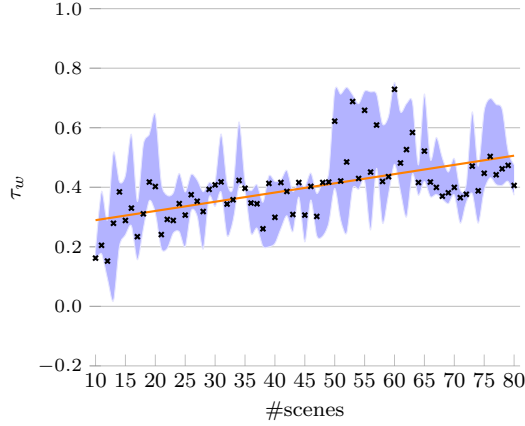


Figure 15: Results for manipulation strategy optimization: τ_w for different numbers of scenes using 100 samples per scene, soft voting, no preference weights, each scene sampled five times with stochastic object pose noise.

Median ($\tilde{\tau}_w$), lower/upper quartile envelope and least-squares best-fit line for 10 training runs.

As for the used voting method, the results in Fig. 14 show a slight improvement of soft over binary voting in terms of mean and variance/positive bias. Therefore we recommend to use soft voting when applying our method. Some improvement is shown also for the number of samples per scene, although this is not surprising since a higher number of samples per individual scene statistically rules out a larger amount of noise.

Summarized, for the following experiment which shows the effectiveness of our self-supervised optimization cycle, we have therefore chosen to use a configuration of *100 samples per scene, soft voting and no injection of preference weights*.

6.2.6 Self-supervised free-time manipulation strategy optimization

With the classifier configuration determined in the last experiment, we ran the whole manipulation strategy optimization cycle in an iterative fashion like in Alg. 4. We started with an initial set of 10 training scenes taken from the total training set as described above. After establishing an initial classifier, one more training scene was generated, a damage-avoiding manipulation sequence planned and the classifier retrained. This was repeated up to a maximum of 80 scenes. Note that, for evaluation purposes, we repeated the classifier training 10 times each with a randomized 2:1 training/testing split on the scenes so as to generate a more noise-resilient evaluation.

The emerging results are shown in Fig. 15 with the median of τ_w over these 10 classifier training runs per scene, further on named $\tilde{\tau}_w$. We added a least-squares best-fit line to $\tilde{\tau}_w$ of each scene which shows a positive slope, hence generally more training data gives better classification results. However, the lower/upper quartile envelope, which initially becomes more narrow, widens again after reaching 50 individual training scenes. Eventually, after 63 scenes, $\tilde{\tau}_w$ drops again well below the best-fit line which indicates overfitting, but recovers

for 75+ scenes.

The given results prove our claim that, while generating more and more training scenes and optimizing the manipulation strategy in a self-supervised manner, there is an improvement in classification accuracy with an increasing number of considered unique scenes. However, it is hard to provide a convergence measure which determines the globally optimal number of scenes after which optimization should be stopped for the scene/object configuration at hand. This strongly depends on the application scenario and the ground truth data for our method has been generated by the method itself. That data includes a certain amount of noise propagating from the low-level motion planning and physics simulation towards the final manipulation strategy which cannot completely be ruled out by our method. Therefore, for a specific application scenario, it is necessary to define some heuristics to determine when exactly to stop the optimization loop and to proceed towards optimizing different scene/object configurations.

In the presented scenario, the τ_w grow sufficiently on their $[-1, 1]$ scale with an increasing number of scenes. Given that -1.0 means full discordance (i.e. the preferences appear in entirely inverse order) and 1.0 means full concordance (i.e. the preference appear in entirely correct order), the τ_w from the classifier predictions are close to the optimal manipulation sequences as determined by mental simulation. This means that not only are the results improving as desired during the optimization process, but they also reflect realistic human-like behavior concerning the respective scene. Hence, our method is able to increase the cognition and reasoning skills of the robot with respect to manipulation preferences.

7 Discussion

In the first part of our work, we presented a mental simulation method to plan manipulation sequences while minimizing potential damage with respect to objects in the scene. This is achieved via anticipating the scene’s dynamics during the interaction process. Moreover, several measures allow for a significant improvement in efficiency. In the second part, we train a classifier that can predict an optimal manipulation sequence from new, unknown scenes. This happens iteratively within a self-supervised manipulation strategy optimization cycle and allows the robot to continuously acquire skills during load-free times. The resulting strategies can be deployed anytime and executed in near-real time.

The presented work merely scratches the surface of what may be possible to infer from physics simulation to create long-term knowledge. However, we were able to show that preferences patterns humans acquire subconsciously get shaped as well in robotic behavior learned via mental simulation. In general, simulation in the loop has not been studied extensively yet in the literature, but has recently been on the rise for problems in the physical reasoning domain, with most authors using the term *mental simulation* [22] like we do.

Bozcuoglu and Beetz [4], for instance, recently proposed a generic simulation setup for knowledge generation and reasoning through mental simulation. However, they do not yet close the loop of propagating the gained knowledge into an optimization cycle. Haidu and Beetz [16] utilize this setup for recognizing and interpreting actions from simulation in order to collect sufficient knowledge about the task for replaying it on a real robot. On the other hand, Levine et al. [30] use up to 14 real manipulators in parallel to collect data for grasp learning. They use visual features combined with a deep learning technique in a parallelized way, making use of massive hardware. This is similar to our approach in a way that parallel randomized experiments are performed in order to generate training data, but different in a way that we do not need to rely on hardware other than computing capacity and try to make use of idle times as far as possible.

Regarding the fidelity of simulation-based planning with respect to the real world, it is a hard problem to design a feature-based physical scene understanding approach based on complex human inferences. It would be necessary to find a set of features which is capable of depicting all inferences humans draw from some input scene using their world knowledge. However, our featureless manipulation sequence planning approach by itself is very resource-demanding during productive use. Hence, the feature-enabled manipulation strategy learning part of our method allows for reducing execution times to a minimum, outsourcing expensive computation into low-load time slots. Strictly speaking, our overall approach proposed herein does not rationalize any mental simulation capabilities, but minorly softens their expressiveness in favor of reasonable use under real-life conditions.

Additionally, vice versa, humans also use certain features as a fallback when scene dynamics are too complex to be anticipated [3]. Hence, the utility of features as a mean of generalization cannot be neglected per se. Nevertheless, it may be possible to increase the overall performance, explicitly precision, of our method when the feature set is iteratively improved based on experimental classification outcomes. The proposed feature set serves as a first attempt to prove the general feasibility and applicability of our approach, although more

investigation is required into adapting the features to the respective use case in productive use. With increased precision, the answer about how to measure converge of the optimization loop may potentially be perfectly obvious.

In any case, in order to avoid permanent retraining of the classifier from scratch, using an online algorithm would improve the temporal performance of our method. With the current setup, retraining the classifier is necessary every time a new training sample has been generated. Although this can happen in parallel to generating the next training sample via mental simulation, updating the classifier in an online fashion removes some computational burden from the approach and allows for faster overall processing, hence shorter time to convergence. Further investigation in terms of speed improvement may prove beneficial for the applicability of the presented method in real-world applications. Future research potentially may also point into the direction of deep learning which generally does not require the developer to define the feature set prior to classifier design. Using this technique, certainly major effort needs to be invested into designing the classifier pipeline. This exceeds the scope of our initial approach to solve the present complex problem and should be investigated in future work.

Nevertheless, a major advantage of the proposed approach is that, except for the feature set, it is almost parameter-free and hence does not require extensive tuning based on the application scenario. The genericness of our approach allows for deployment in many different scenarios for which a simulation of the robot and scene dynamics can be provided. Therefore, the method can easily be integrated into existing applications as a mean of high-level task planning including the capability of self-supervised strategy optimization.

References

- [1] Abdel-Malek, K., Yang, J., Blackmore, D., Joy, K.: Swept Volumes: Fundation [*sic*], Perspectives, and Applications. *International Journal of Shape Modeling* **12**(1) (2006)
- [2] Akbari, A., Gillani, M., Rosell, J.: Task and Motion Planning Using Physics-based Reasoning. In: *International Conference on Emerging Technologies and Factory Automation* (2015)
- [3] Battaglia, P., Hamrick, J., Tenenbaum, J.: Simulation as an engine of physical scene understanding. *Proceedings of the National Academy of Sciences of the United States of America* **110**(45), 18,327–32 (2013)
- [4] Bozcuoglu, A.K., Beetz, M.: A Cloud Service for Robotic Mental Simulations. In: *International Conference on Robotics and Automation* (2017)
- [5] Burges, C., Shaked, T., Renshaw, E., Lazier, A., Deeds, M., Hamilton, N., Hullender, G.: Learning to Rank using Gradient Descent. In: *International Conference on Machine Learning*, pp. 89–96 (2005)
- [6] le Cessie, S., van Houwelingen, J.: Ridge estimators in logistic regression. *Applied Statistics* **41**(1), 191–201 (1992)
- [7] Cheng, W., Huehn, J., Huellermeier, E.: Decision Tree and Instance-Based Learning for Label Ranking. In: *International Conference on Machine Learning* (2009)

- [8] Dogar, M., Hsiao, K., Ciocarlie, M., Srinivasa, S.: Physics-Based Grasp Planning Through Clutter. In: *Robotics: Science and Systems* (2012)
- [9] von Driegielewski, A., Hemmer, M., Schoemer, E.: High Precision Conservative Surface Mesh Generation for Swept Volumes. *Transactions on Automation Science and Engineering* **12**(1), 764–769 (2015)
- [10] Fischinger, D., Weiss, A., Vincze, M.: Learning Grasps with Topographic Features. *International Journal of Robotics Research* **34**(9), 1167–1194 (2015)
- [11] Fromm, T., Birk, A.: Physics-Based Damage-Aware Manipulation Strategy Planning Using Scene Dynamics Anticipation. In: *International Conference on Intelligent Robots and Systems* (2016)
- [12] Fromm, T., Mueller, C.A., Birk, A.: Unsupervised Watertight Mesh Generation From Noisy Free-Form RGBD Object Models Using Growing Neural Gas. Tech. rep., Jacobs University (2016). <https://arxiv.org/abs/1603.00663>
- [13] Fromm, T., Mueller, C.A., Pfingsthorn, M., Birk, A., Di Lillo, P.: Efficient Continuous System Integration and Validation for Deep-Sea Robotics Applications. In: *Oceans* (2017)
- [14] Goldberg, K.: Stochastic Plans for Robotic Manipulation. Ph.D. thesis (1990)
- [15] Grbovic, M., Djuric, N., Vucetic, S.: Learning from Pairwise Preference Data using Gaussian Mixture Model. In: *Preference Learning Workshop, European Conference on Artificial Intelligence* (2012)
- [16] Haidu, A., Beetz, M.: Action recognition and interpretation from virtual demonstrations. In: *International Conference on Intelligent Robots and Systems*, pp. 2833–2838 (2016)
- [17] Hangl, S., Ugur, E., Szedmak, S., Piater, J.: Robotic Playing for Hierarchical Complex Skill Learning. In: *International Conference on Intelligent Robots and Systems* (2016)
- [18] Huellermeier, E., Fuernkranz, J.: Ranking by Pairwise Comparison: A Note on Risk Minimization. In: *International Conference on Fuzzy Systems* (2004)
- [19] Huellermeier, E., Fuernkranz, J., Cheng, W., Brinker, K.: Label Ranking by Learning Pairwise Preferences. *Artificial Intelligence* **172**(16-17) (2008)
- [20] Joachims, T.: Optimizing Search Engines using Clickthrough Data. In: *Conference on Knowledge Discovery and Data Mining* (2002)
- [21] Joachims, T.: Training Linear SVMs in Linear Time. In: *Conference on Knowledge Discovery and Data Mining* (2006)
- [22] Kahneman, D., Tversky, A.: The Simulation Heuristic. Tech. rep., Stanford University, Department of Psychology (1981)

- [23] Kappler, D., Bohg, J., Schaal, S.: Leveraging Big Data for Grasp Planning. In: International Conference on Robotics and Automation, pp. 4304–4311 (2015)
- [24] Katz, D., Venkatraman, A., Kazemi, M., Bagnell, J.A., Stentz, A.: Perceiving, Learning, and Exploiting Object Affordances for Autonomous Pile Manipulation. In: Robotics: Science and Systems (2013)
- [25] Kendall, M.: A new measure of rank correlation. *Biometrika* **30**(1/2), 81–93 (1938)
- [26] Kitaev, N., Mordatch, I., Patil, S., Abbeel, P.: Physics-Based Trajectory Optimization for Grasping in Cluttered Environments. In: International Conference of Robotics and Automation (2015)
- [27] Kluth, T., Burigo, M., Knoefler, P.: Shifts of Attention During Spatial Language Comprehension: A Computational Investigation. In: International Conference on Agents and Artificial Intelligence (2016)
- [28] Kumar, R., Vassilvitskii, S.: Generalized Distances between Rankings. In: International Conference on World Wide Web (2010)
- [29] Kunze, L., Beetz, M.: Envisioning the qualitative effects of robot manipulation actions using simulation-based projections. *Artificial Intelligence* (2015)
- [30] Levine, S., Pastor, P., Krizhevsky, A., Quillen, D.: Learning Hand-Eye Coordination for Robotic Grasping with Deep Learning and Large-Scale Data Collection. In: International Symposium on Experimental Robotics (2016)
- [31] Li, W., Leonardis, A., Fritz, M.: Visual Stability Prediction for Robotic Manipulation. In: International Conference on Robotics and Automation, pp. 2606–2613 (2017)
- [32] Merkel, D.: Docker: Lightweight Linux Containers for Consistent Development and Deployment. *Linux Journal* **2014**(239) (2014)
- [33] Mojtahedzadeh, R., Bouguerra, A., Schaffernicht, E., Lilienthal, A.: Support relation analysis and decision making for safe robotic manipulation tasks. *Robotics and Autonomous Systems* **71**(July 2015), 99–117 (2015). <https://github.com/Rasoul77/promts>
- [34] Mojtahedzadeh, R., Lilienthal, A.: A Principle of Minimum Translation Search Approach for Object Pose Refinement. In: International Conference on Intelligent Robots and Systems (2015)
- [35] Morgan, S., Branicky, M.: Sampling-Based Planning for Discrete Spaces. In: International Conference on Intelligent Robots and Systems (2004)
- [36] Mottaghi, R., Rastegari, M., Gupta, A., Farhadi, A.: "What happens if..." Learning to Predict the Effect of Forces in Images. In: European Conference on Computer Vision (2016)

- [37] Mueller, C.A., Pathak, K., Birk, A.: Object Shape Categorization in RGBD Images using Hierarchical Graph Constellation Models based on Unsupervisedly Learned Shape Parts described by a Set of Shape Specificity Levels. In: International Conference on Intelligent Robots and Systems (2014)
- [38] Okada, K., Haneda, A., Nakai, H., Inaba, M., Inoue, H.: Environment Manipulation Planner for Humanoid Robots Using Task Graph That Generates Action Sequence. In: International Conference on Intelligent Robots and Systems (2004)
- [39] Panda, S., Hafez, A., Jawahar, C.: Learning Support Order for Manipulation in Clutter. In: International Conference on Intelligent Robots and Systems (2013)
- [40] Pastor, P., Kalakrishnan, M., Chitta, S., Theodorou, E., Schaal, S.: Skill learning and task outcome prediction for manipulation. In: International Conference on Robotics and Automation (2011)
- [41] Peshkin, M., Sanderson, A.: Planning Robotic Manipulation Strategies for Sliding Objects. In: International Conference on Robotics and Automation, vol. 4, pp. 696–701 (1987)
- [42] Regier, T., Carlson, L.: Grounding Spatial Language in Perception: An Empirical and Computational Investigation. *Journal of Experimental Psychology: General* **130**(2), 273–298 (2001)
- [43] Rockel, S., Konecny, S., Stock, S., Hertzberg, J., Pecora, F., Zhang, J.: Integrating Physics-Based Prediction with Semantic Plan Execution Monitoring. In: International Conference on Intelligent Robots and Systems (2015)
- [44] de Sa, C.R., Soares, C., Knobbe, A., Cortez, P.: Label Ranking Forests. *Expert Systems* **34**(1), 1–8 (2017)
- [45] Schwarz, G.: Estimating the dimension of a model. *Annals of Statistics* **6**(2), 461–464 (1978)
- [46] Shalev-Shwartz, S., Singer, Y.: Efficient Learning of Label Ranking by Soft Projections onto Polyhedra. *Journal of Machine Learning Research* **7**, 1567–1599 (2006)
- [47] Sjöö, K., Jensfelt, P.: Learning spatial relations from functional simulation. In: International Conference on Intelligent Robots and Systems (2011)
- [48] Stilman, M., Schamburek, J.U., Kuffner, J., Asfour, T.: Manipulation Planning Among Movable Obstacles. In: International Conference on Robotics and Automation (2007)
- [49] Stoyanov, T., Vaskevicius, N., Mueller, C.A., Fromm, T., Krug, R., Tincani, V., Mojtahedzadeh, R., Kunaschk, S., Mortensen Ernits, R., Ricao Canelhas, D., Bonilla, M., Schwertfeger, S., Bonini, M., Halfar, H., Pathak, K., Rohde, M., Fantoni, G., Bicchi, A., Birk, A., Lilienthal, A., Echelmeyer, W.: No More Heavy Lifting: Robotic Solutions to the Container Unloading Problem. *Robotics and Automation Magazine* **23**(4) (2016)

- [50] Sucan, I., Moll, M., Kavraki, L.: The Open Motion Planning Library. *Robotics & Automation Magazine* **19**(4), 72–82 (2012)
- [51] Sutton, C., McCallum, A.: An Introduction to Conditional Random Fields. *Machine Learning* **4**(4), 267–373 (2011)
- [52] Taeubig, H., Baeuml, B., Frese, U.: Real-time Swept Volume and Distance Computation for Self Collision Detection. In: *International Conference on Intelligent Robots and Systems* (2011)
- [53] Vaskevicius, N., Mueller, C.A., Bonilla, M., Tincani, V., Stoyanov, T., Fantoni, G., Pathak, K., Lilienthal, A., Bicchi, A., Birk, A.: Object Recognition and Localization for Robust Grasping with a Dexterous Gripper in the Context of Container Unloading. In: *International Conference on Automation Science and Engineering* (2014)
- [54] Vaskevicius, N., Pathak, K., Birk, A.: Fitting Superquadrics in Noisy , Partial Views from a Low-cost RGBD Sensor for Recognition and Localization of Sacks in Autonomous Unloading of Shipping Containers. In: *International Conference on Automation Science and Engineering* (2014)
- [55] Vaskevicius, N., Pathak, K., Ichim, A., Birk, A.: The Jacobs Robotics approach to object recognition and localization in the context of the ICRA’11 Solutions in Perception Challenge. In: *International Conference on Robotics and Automation* (2012)
- [56] Weisz, J., Allen, P.: Pose Error Robust Grasping from Contact Wrench Space Metrics. In: *International Conference on Robotics and Automation* (2012)
- [57] Weitnauer, E., Haschke, R., Ritter, H.: Evaluating a Physics Engine as an Ingredient for Physical Reasoning. In: *International Conference on Simulation, Modeling, and Programming for Autonomous Robots* (2010)
- [58] Winkler, J., Balint-Benczedi, F., Wiedemeyer, T., Beetz, M., Vaskevicius, N., Mueller, C.A., Fromm, T., Birk, A.: Knowledge-Enabled Robotic Agents for Shelf Replenishment in Cluttered Retail Environments. In: *International Conference on Autonomous Agents and Multiagent Systems* (2016)
- [59] Xing, Z., Pei, J., Keogh, E.: A Brief Survey on Sequence Classification. *ACM SIGKDD Explorations Newsletter* **12**(1), 40 (2010)
- [60] Zhou, Y., Liu, Y., Gao, X.Z., Qiu, G.: A label ranking method based on Gaussian mixture model. *Knowledge-Based Systems* **72**, 108–113 (2014)